

Constant fields and constant gradients in open ionic channels

Duan Pin Chen, Victor Barcion, and Robert S. Eisenberg
Department of Physiology, Rush Medical Center, Chicago, Illinois 60612 USA

ABSTRACT Ions enter cells through pores in proteins that are holes in dielectrics. The energy of interaction between ion and charge induced on the dielectric is many kT , and so the dielectric properties of channel and pore are important. We describe ionic movement by (three-dimensional) Nernst-Planck equations (including flux and net charge). Potential is described by Poisson's equation in the pore and Laplace's equation in the channel wall, allowing induced but not permanent charge. Asymptotic expansions are constructed exploiting the long narrow shape of the pore and the relatively high dielectric constant of the pore's contents. The resulting one-dimensional equations can be integrated numerically; they can be analyzed when channels are short or long (compared with the Debye length). Traditional constant field equations are derived if the induced charge is small, e.g., if the channel is short or if the total concentration gradient is zero. A constant gradient of concentration is derived if the channel is long. Plots directly comparable to experiments are given of current vs. voltage, reversal potential vs. concentration, and slope conductance vs. concentration. This dielectric theory can easily be tested: its parameters can be determined by traditional constant field measurements. The dielectric theory then predicts current-voltage relations quite different from constant field, usually more linear, when gradients of total concentration are imposed. Numerical analysis shows that the interaction of ion and channel can be described by a mean potential if, but only if, the induced charge is negligible, that is to say, the electric field is spatially constant.

INTRODUCTION

Classical theories of electrodiffusion describe structures with fixed geometry, for example, channels with a definite length and cross-sectional area (constant field theory: Goldman, 1943; Hodgkin and Katz, 1949; liquid junction theory: Henderson, 1907, 1908; MacInnes, 1961). Electrodiffusion through the membranes of cells occurs, however, through a varying number of different kinds of channels, in effect, through a varying cross-sectional area of different sorts of permeable membrane (Hille, 1984). Indeed, the macroscopic movement of substances is often controlled by opening and closing channels, thereby changing the area and kind of membrane through which a particular ion can move. Such macroscopic fluxes, flowing through varying numbers (typically, tens of thousands) and types of (typically, two to ten) channels cannot be described by the classical equations of electrodiffusion, because those assume a fixed area of membrane available for ionic movement.

Microscopic currents flowing through a single channel are quite different from macroscopic currents flowing through many channels. Once a particular channel is open, its geometry is presumably fixed and the microscopic current flows through a definite area, constant in

time. Classical theories of electrodiffusion originally described currents in gross preparations of many cells; they fell out of favor as the voltage clamp was used to measure currents in small but macroscopic pieces of membrane from single cells (Hodgkin, 1971, 1977). They are needed once again to codify, understand, and perhaps guide these measurements, now that currents are routinely measured in submicroscopic pieces of those membranes, namely single open channels.

Constant field theory (Goldman, 1943; Hodgkin and Katz, 1949) is widely used for such analysis but often with some confusion between its original macroscopic derivation and its present microscopic application. Many papers have analyzed electrodiffusion in a macroscopic context (in several fields, viz., membrane biophysics: Adrian, 1969; Läuger and Neumcke, 1973; Sten-Knudsen, 1978; electrochemistry: Buck, 1984; Rubinstein, 1990; semiconductor physics: Selberherr, 1984; Markowich, 1986; Hess, 1988; electron transport in metals: Verhoeven, 1963), but reexamination seems necessary before classical theories are used to describe ionic movement through channels of atomic size.

Cooper, Gates, and Eisenberg (1988; following many others in the biological literature, e.g., Levitt, 1982, 1986; Jordan, 1987) describe ionic movement as a diffusive process, arguing (following many in the chemical literature, e.g., Murthy and Singer, 1987) that solute

Dr. Barcion's other address is Departments of Mathematics and Geophysical Sciences, University of Chicago, 5734 South Ellis, Chicago, IL 60636.

movement on the biological time scale of microseconds to seconds involves a large number ($> 10^3$) of collisions between atoms, even in the shortest time likely to be relevant to permeation (10^{-7} s). Such movement is described by classical continuum equations: the Nernst-Planck equations (as used by Planck, 1890a,b; Henderson, 1907, 1908; MacInnes, 1961; Goldman, 1943; Hodgkin and Katz, 1949; Levitt, 1982, 1986; Jordan, 1987) describe average properties; Fokker-Planck equations (Cooper et al., 1988) describe stochastic properties, as do the more or less equivalent stochastic differential equations, the Langevin equations (Cooper, Jakobsson, and Wolynes, 1985) that describe trajectories of individual particles drifting and randomly walking through a potential field. Classical Nernst-Planck equations are one-dimensional, not describing a channel at all. They can easily be scaled to describe one-dimensional flow across an area and through a length of a channel. But no trace of the induced charge or dielectric properties of the channel protein appear in the equations. Classical Nernst-Planck equations do not allow interaction between ion and channel wall and so are hard to justify as a description of ionic movement through biological channels, which are just 0.6–1.5 nm in diameter, comparable to a Debye length, the length scale of interaction between charges in solutions. Thus, electrical interaction is expected to occur; indeed, it is hard to see how the biological properties of a channel (e.g., selectivity, rectification, and gating) could occur without such interaction.

Many workers have modified the classical Nernst-Planck equations to include interactions (following Neumcke and Lauger, 1969) between ion and channel, describing ion-channel interactions as a charge interacting with a mean potential, a potential dependent on location but independent of all other parameters, including time, dielectric constant, concentration, and current.¹ A similar treatment is used in stochastic analysis of Fokker-Planck equations (following Kramers, 1940; further references in Cooper et al., 1988) and Langevin equations (references in Cooper et al., 1985), and in much of solid state physics (e.g., Hess, 1988; Markowich, 1986; Selberherr, 1984). In these theories, the interaction of matter and a charge is described by a potential, an energy, sometimes called “the potential of mean force.” That energy is assumed constant, known in advance, independent of the parameters of the theory, the same for every concentration gradient, flux, and diffusion constant of each ion in the pore.

¹The interaction should not be computed with image charge methods, because those methods are not general and do not permit solution of Maxwell's or Poisson's equations in most geometries, e.g., a finite cylinder (Panofsky and Phillips, 1962, pp. 39–43).

The difficulty with this description is that it is in conflict with the electrical properties of matter as described by Maxwell's equations. Ions do indeed interact with a surface potential as they flow through a channel, but that potential depends on all the parameters of the problem,² e.g., the type, location, and amount of ions in the pore. The ions in a pore are anything but constant; thus, it is unwise to assume that an ion interacts with a fixed potential when it in fact interacts with matter. Such could be an end, but should not be a beginning of analysis.

The mean potential approach fails because the force between an ion and matter cannot be described as the interaction of an ion with a fixed preordained potential. Matter itself is made of internal charges that move in response to an electric field or a nearby ion, creating significant induced charge, even if the matter is originally uniform and electrically neutral, and even if the induced movement of charges inside the matter is tiny. Tiny movements produce significant polarization charge inside and on the surface of matter, thus producing its dielectric properties. These dielectric properties are always important, usually dominant determinants of the energetics and movement of ions near proteins in solution because an ion is so close (i.e., < 0.2 nm) to the atoms of water and the channel wall. Estimates of the energy of interaction between an ion and dielectric (Eqs. 3.8–3.10 in Israelachvili, 1985) show that dielectric interactions depend on the difference in the reciprocal of the dielectric constants and are very strong, easily tens of kT in energy (using parameters in Table 1; and Eq. 3.10 in Israelachvili, 1985). Currents through channels often depend exponentially on the interaction energy (divided by kT); thus, the dielectric properties of the channel wall and pore must be explicitly (and accurately) included in a theory of permeation. Approximations that neglect dielectric effects are inherently implausible and require mathematical or physical justification, in our view.

Here we develop a theory of electrodiffusion in channels allowing only the simplest electrical interaction between channel wall and permeating ion, the interaction between a charge and a dielectric, seeking formulae describing current flow through an open channel, directly comparable to experimental data. We find some

²More precisely, the interaction of an ion with a fixed potential is described in electrostatics by a “Dirichlet boundary condition” and is quite different from the interaction of an ion with matter, which is described by a “jump boundary condition” (Panofsky and Phillips, 1962, p. 32). It would be a mathematical miracle if the two quite different boundary conditions gave the same physical forces over a range of concentrations, fluxes, and diffusion constants of each ion in the pore.

cases where dielectric interactions dominate the theory and other cases where they are negligible. We try to set the stage for a more precise analysis, that would use the actual (local) dielectric properties and permanent charge distribution of channel proteins, once they are measured or computed from realistic simulations of atomic dynamics (Brooks, Karplus, and Pettit, 1988; McCammon and Harvey, 1987).

THEORY

Readers primarily interested in using this theory may prefer to turn directly to Eq. 19.

Statement of problem. Equations must be written in three dimensions if the dielectric properties of the channel are to be analyzed: we do not know how (*a priori*) to describe dielectric interactions in one dimension, where dielectric and pore would occupy the same space. The open channel is described by the Nernst-Planck equations, with flux \vec{J}_i which satisfies the continuity equation

$$\nabla \cdot \vec{J}_i = 0. \quad (1)$$

The flux \vec{J}_i ($\text{cm}^{-2} \cdot \text{s}^{-1}$) of each ion i is

$$\vec{J}_i = -D_i \left[\nabla c_i + \frac{Z_i e}{kT} c_i \nabla \varphi \right], \quad (2)$$

where $c_i(r, x, \theta)$ (units: cm^{-3}) is the concentration of species i ; $\varphi(r, x, \theta)$ is the electrical potential in volts; Z_i is the charge on each ion, positive for cations, negative for anions in units of e , the charge on the proton, $1.6 \cdot 10^{-19}$ coulomb; k is Boltzmann's constant, and T is the absolute temperature; D_i is the diffusion constant (cm^2/s) of the i th ion in the channel's pore. This diffusion constant may be very different from the value in bulk solution, because the environment of an ion in a pore is very different. D_i is assumed independent of x . The x dependent case could be handled without much difficulty, at least numerically, if the dependence were known from, for example, simulations of the molecular dynamics of ion permeation.

The potential φ arises from the distribution of the charge $\sum_i Z_i e c_i$ on ions free to move macroscopic distances and from the distribution of charge bound to molecules, able only to move atomic distances. Bound charge can be a permanent chemical property of an atom or molecule, independent of the local electric field, or it can be induced by the local electric field, being zero when that field is zero and proportional to that field in other cases (Purcell, 1985, chapter 10, particularly pp. 388 and 389; Feynmann, Leighton, and Sands, 1964, chapter 10 and 32). Here all the bound charge is assumed to be induced, described by the polarization field, proportional to the electric field, with the proportionality constant truly constant, independent of time or location (or potential, current, or concentration, for that matter), equal to $\epsilon_a - \epsilon_o$, where $\epsilon_o = 88.5$ fF/cm is the permittivity of free space and ϵ_a is the permittivity of the pore of the channel. $\epsilon_a = \epsilon_{ra} \cdot \epsilon_o$, where ϵ_{ra} is the relative permittivity, i.e., dielectric constant. The electric field is described by Poisson's equation:

$$\nabla^2 \varphi = -\frac{1}{\epsilon_{ra} \epsilon_o} \sum_i Z_i e c_i. \quad (3)$$

A dielectric theory should allow the proportionality constant to depend on time and location once that dependence is known experi-

mentally or from simulations of molecular dynamics. A cylindrical coordinate system (r, x, θ) is used, but axial symmetry is assumed so there is no θ dependence. Outside the pore, but still in the channel protein, no ions are present and so the potential is described by Laplace's equation

$$\nabla^2 \varphi = 0. \quad (4)$$

The potential on the left hand side is assumed to be $\varphi(x=0) = V$, to be specific, where we choose the origin of the longitudinal coordinate x ; d is the channel length. The potential outside (on the right hand side) is assumed zero, $\varphi(x=d) = 0$, positive flux and current is assumed outward (from left to right), and the concentration of each ion is described by

$$c_i(x=0) = l_i \cdot c_L \quad \text{on the left hand side} \quad (5)$$

and

$$c_i(x=d) = r_i \cdot c_R \quad \text{on the right hand side.} \quad (6)$$

Electrical neutrality is assumed on each side of the channel (but not within the pore), so on the left hand side

$$\sum_{Z_i > 0} l_i Z_i = -\sum_{Z_i < 0} l_i Z_i = 1 \quad (7)$$

and on the right hand side

$$\sum_{Z_i > 0} r_i Z_i = -\sum_{Z_i < 0} r_i Z_i = 1. \quad (8)$$

The potential within the pore is linked to the potential within the channel protein by dielectric boundary conditions

$$\varphi(a-0, x) = \varphi(a+0, x) \quad (9)$$

$$\frac{\partial \varphi}{\partial r}(a-0, x) = \epsilon \frac{\partial \varphi}{\partial r}(a+0, x). \quad (10)$$

$a-0$ means a location just inside the channel wall and $a+0$ means just outside the channel wall; ϵ is the ratio of permittivities (equivalently, ratio of dielectric constants) of the channel wall ϵ_m and aqueous solutions ϵ_a .

$$\epsilon = \frac{\epsilon_m}{\epsilon_a}. \quad (11)$$

These equations assume no permanent (i.e., independent of $\nabla \varphi$) surface charge on the channel wall. In this paper we only consider induced charge, namely polarization charge proportional to the local electric field, leaving the analysis of permanent charge until another time.

Ions are confined to the pore by forbidding radial flux at the wall of the channel $r = a$

$$\frac{\partial c_i(a, x)}{\partial r} + \frac{Z_i e}{kT} \cdot c_i(a, x) \cdot \frac{\partial \varphi(a, x)}{\partial r} = 0. \quad (12)$$

The measured experimental variable is the current $I(V)$ flowing out of the channel mouth, the spatial integral, nearly the spatial average of the fluxes

$$I(V) = \sum_i (e Z_i) (2\pi) \int_0^a \vec{J}_i(r, d) \cdot \hat{r} \, r \, dr, \quad (13)$$

where $\hat{\mathbf{r}}$ is the radial unit vector. Our intuition has been aided by displaying the induced charge $\sigma_{\text{pol}}(x)$ along the cylindrical surface of the channel, once $\varphi(r, x)$ is determined (Panofsky and Phillips, 1962, p. 32).

$$\frac{\sigma_{\text{pol}}}{\epsilon_0} = \frac{\partial \varphi}{\partial r}(a - 0, x) - \frac{\partial \varphi}{\partial r}(a + 0, x). \quad (14)$$

An asymptotic analysis (Kevorkian and Cole, 1981) of these coupled nonlinear partial differential equations (1–10) can be found in Barcilon et al. (1991). There the three-dimensional problem is reduced to a one-dimensional problem by exploiting the small ratio α of diameter to length of channels, using the distinguished limit where $\epsilon = (-\alpha^2 \ln \alpha) \bar{\epsilon}$. The results are expressed in the nondimensional spatial variable z , and the nondimensional potentials $\phi(r, z)$:

$$\alpha = \frac{a}{d}; \quad \bar{\epsilon} = \frac{\epsilon}{-\alpha^2 \ln \alpha}; \quad z = \frac{x}{d};$$

$$\phi(r, z) = \varphi(r, z) \cdot e/kT. \quad (15)$$

The analysis shows that the leading term of the expansions for the flux J_i is independent of position, and the leading terms $\Phi(z)$ and $C_i(z)$ of the expansions for the potential $\varphi(r, z)$ and concentrations $c_i(r, z)$ depend only on axial location. The Appendix shows how these variables also describe the spatial average of the potential and concentration in channels of varying cross-section, perhaps not long and narrow, although the error terms are not evaluated in that case.

$$\begin{aligned} \phi(r, z) &= \Phi(z) + o(1) \\ c_i(r, z) &= C_i(z) + o(1) \\ \tilde{J}_i(r, z) &= J_i + o(1), \text{ in the } z \text{ direction.} \end{aligned} \quad (16)$$

The order notation $o(1)$ (“little oh one”: see Olver, 1974, pp. 4–11), describes the error terms in the expansions of Barcilon et al. roughly

The ionic strength \hat{I}_c (units: cm^{-3}) in the present treatment is computed from the ionic strength in either the left or right hand bath.³

$$\begin{aligned} I_c(\text{L}) &= \frac{1}{2} C_{\text{L}} \sum_i I_i Z_i^2; \\ I_c(\text{R}) &= \frac{1}{2} C_{\text{R}} \sum_i r_i Z_i^2. \end{aligned} \quad (18)$$

When computing the numerical solution of the differential equations, we chose $\hat{I}_c = \frac{1}{2}[I_c(\text{L}) + I_c(\text{R})]$; when using the constant field expressions, it would be better to choose $\hat{I}_c = \max [I_c(\text{L}); I_c(\text{R})]$; when computing the constant gradient expression, it would be better to choose $\hat{I}_c = \min [I_c(\text{L}); I_c(\text{R})]$.

The system of one-dimensional differential equations (written here for three univalent ions $Z_1 = 1, Z_2 = 1, Z_3 = -1$) is

$$\begin{aligned} \frac{dC_1}{dz} + C_1 \cdot \frac{d\Phi}{dz} &= -J_1 d/D_1 \\ \frac{dC_2}{dz} + C_2 \cdot \frac{d\Phi}{dz} &= -J_2 d/D_2 \\ \frac{dC_3}{dz} - C_3 \cdot \frac{d\Phi}{dz} &= -J_3 d/D_3. \end{aligned} \quad (19)$$

The role of the fluxes and diffusion constants $J_i d/D_i$ in these equations is interesting. They are constants, independent of location and time in this steady-state problem; in a way they are integration constants of the differential equations. Once the differential equations (19) are multiplied by an integrating factor and explicitly integrated (as shown in Eq. 6 of Barcilon et al., 1991), the integration constants, i.e., the flux terms $J_i d/D_i$, are determined by the boundary conditions 5–8, leaving expressions for the concentration C_i that do not depend on the diffusion constants or fluxes at all (Eq. 5.7 of Barcilon et al., 1991).

The asymptotic analysis yields an equation for the potential within the channel, also independent of flux or diffusion constant.

$$\frac{d^2 \Phi(z)}{dz^2} + \underbrace{2 \frac{\epsilon}{\alpha^2 \ln \alpha} (\Phi(z) - [1 - z] \Delta)}_{\text{dielectric correction: induced charge}} = -\lambda^2 \underbrace{\frac{C_1(z) + C_2(z) - C_3(z)}{\hat{I}_c}}_{\text{space charge}}. \quad (20)$$

meaning “smaller than order one, as $\alpha \rightarrow 0$.” The Discussion describes what little can be said in general about the error involved in using just the first term of the expansion. The transmembrane potential V is described by the dimensionless variable Δ ; the dimensionless variable λ describes the effective length, the relative size of the channel length d , and the Debye length κ^{-1} that is the width of the ionic atmosphere

$$\begin{aligned} \Delta &= \frac{e}{kT} V; \\ \lambda &= \kappa d, \end{aligned}$$

where

$$\kappa^2 = \frac{e^2 \hat{I}_c}{\epsilon_{\text{ar}} \epsilon_0 \cdot kT}. \quad (17)$$

The boundary conditions at $z = 0$ and $z = 1$ are

$$\begin{array}{cc} z = 0 & z = 1 \\ \overbrace{C_1(0) = l C_{\text{L}}} & \overbrace{C_1(1) = r C_{\text{R}}} \\ \overbrace{C_2(0) = (1 - l) C_{\text{L}}} & \overbrace{C_2(1) = (1 - r) C_{\text{R}}} \\ \overbrace{C_3(0) = C_{\text{L}}} & \overbrace{C_3(1) = C_{\text{R}}} \\ \overbrace{\Phi(0) = \Delta = eV/kT} & \overbrace{\Phi(1) = 0.} \end{array} \quad (21)$$

³In our theory the ionic strength is simply used to define a length scale. We are aware that fluxes in other electrochemical systems can be large enough to change ionic strength in some locations and thus produce a variable, spatially dependent, and nonlinear scaling into perturbation expansions (Rubinstein, 1990, pp. 3 and 107).

Eqs. 19 and 21 are the classical one-dimensional Nernst-Planck equations. What is not classical is their coupling through a modified version of the Poisson equation, relating the violation of electrical neutrality (i.e., the space charge) $C_1(z) + C_2(z) - C_3(z)$ to the electric field (Eq. 20).

The differential Eqs. 19–21 with two point boundary conditions have been solved numerically with a commercially available multiple shooting procedure (BVMP; Sewel, 1982; Press et al., 1986). Their numerical solutions were within machine error of solutions of the equivalent integral equation (Barcilon et al., 1991), and were indistinguishable from constant field, or constant gradient approximations in the appropriate regimes. Computation of the potential and concentration profiles for one set of parameters at 500 spatial points and an iteration accuracy of 10^{-9} took less than 2 s, using an IBM RS/6000, model 320 (Austin, TX).

Induced charge

The induced charge $\sigma_{\text{pol}}(z)$ (units: coulomb/cm²) along the cylindrical surface of the channel can be determined from Eq. 14 and Eqs. 5.14 and 5.9 of Barcilon et al. (1991). Note that $\sigma_{\text{pol}}(z)$ is proportional to the dielectric correction term $\mathcal{S}(z, \Delta) \equiv \Phi(z) - [1 - z]\Delta$ of Eq. 20:

$$\sigma_{\text{pol}}(z) = \frac{\epsilon_0 kT}{a} \frac{1}{e \ln \alpha} (\Phi(z) - [1 - z]\Delta). \quad (22)$$

We see then that deviations $\mathcal{S}(z, \Delta)$ from constant field $[1 - z]\Delta$, are tied to the amount of induced surface charge (see Eq. 59).⁴ When the induced surface charge is negligible, the potential gradient will be linear and the second derivative will be zero. Then, the dielectric correction term drops out of the modified Poisson equation (20), i.e., $\sigma_{\text{pol}}(z) = 0$ and the space charge $\lambda^2(C_1(z) + C_2(z) - C_3(z))$ is also zero.

Profiles of concentration and potential. The fact that the concentration profiles do not depend on the diffusion constants of ions, in the bulk or in the pore, has interesting physical consequences. In our theory, ions are distinguished chiefly by their diffusion constants in the pore; different ions of the same charge are hardly otherwise recognizable, except, of course, by their different concentrations. Thus, it is perhaps not too surprising that many key results concerning the potential and concentration profiles (e.g., Eqs. 23 and 39–41) depend on the total concentration of ions and not on the individual ion concentration. The individual ion concentrations become critically important only when we measure flux or current, or functions of them, because only then do the diffusion constants of individual ions in the pore, that distinguish ions one from another, enter prominently into our expressions (e.g., Eqs. 27–31). Those parameters influence the time course by which the concentration profiles are established but they do not influence the steady-state profile itself (Cohen and Cooley, 1965; Cole, 1965, 1968; Mafé, Manzanaes, and Pellicer, 1988).

Simplifications of the one-dimensional expansion. The one-dimensional version (Eqs. 19–21) can be further simplified (*case 1*) if the

⁴Note that classical analyses of liquid junctions and constant fields are not consistent with the usual (uncorrected) equations of the electric field. For example, a constant field implies electrical neutrality yet computation of the space charge from the constant field theory (i.e., Eqs. 24–26) does not yield zero, i.e., electrical neutrality (Bass, 1964; Zelman, 1968; MacGillivray, 1968; MacGillivray and Hare, 1969; Friedman, 1969; Zelman and Shih, 1972; Jackson, 1974; Mafé, Pellicer, and Aguilera, 1986; Riveros, Croxton, and Armstrong, 1989). Consistency requires a modification of the constant field or of Poisson's equation along the lines of our equation (20).

channel is short ($\lambda^2 \ll 1$) compared with the ionic atmosphere; (*case 2*) if the channel is long ($\lambda^2 \gg 1$) compared with the ionic atmosphere; (*case 3*) if the concentrations are symmetrical with $r = l$; (*case 4*) if the diffusion constants of different ions in the pore are identical $D_i = D$; (*case 5*) if the gradient of total ion concentration is small, namely $(C_L - C_R) \rightarrow 0$; (*case 6*) if the ratio of dielectric constants $\epsilon \approx 1$. Under physiological conditions, with ionic strength $I_c \approx 150 \text{ mM} \approx 9 \times 10^{19} \text{ cm}^{-3}$, and dielectric constants $\epsilon_a = 80$, $\epsilon_m = 2$, the ionic atmosphere is probably some 1-nm thick, with the channel being from 3 to 10 nm long, so we anticipate the long channel case (2) to be the most relevant to biological channels.

Simplifications: (case 1) short channels with constant electric fields. Expanding Eqs. 19–21 in powers of λ^2 gives the constant field expression (Cole, 1965, 1968), and the corresponding induced charge

$$\Phi(z) = \Delta(1 - z) = \frac{d - x}{d} \cdot \frac{eV}{kT}; \quad \sigma_{\text{pol}}(z) = 0. \quad (23)$$

The next order problem for Φ in this expansion has been solved for a special case but is not presented because direct comparison with the numerical solution of the integral or differential equation is more general and accurate.

The corresponding distribution of concentration within the pore is

$$C_1(z) = \frac{rC_R[e^{zeV/kT} - 1] + lC_L[e^{eV/kT} - e^{zeV/kT}]}{e^{eV/kT} - 1} \quad (24)$$

$$C_2(z) = \frac{(1 - r)C_R[e^{zeV/kT} - 1] + (1 - l)C_L[e^{eV/kT} - e^{zeV/kT}]}{e^{eV/kT} - 1} \quad (25)$$

$$C_3(z) = \frac{C_R[e^{-zeV/kT} - 1] + C_L[e^{-eV/kT} - e^{-zeV/kT}]}{e^{-eV/kT} - 1}. \quad (26)$$

These equations show that the distribution of concentration within the pore in this approximation is independent of many parameters of the problem. It is independent of the diffusion constants of ions in the pore in general. In both the constant field and constant gradient approximations, it is also independent of the dielectric constant of the pore and channel protein, and of the aspect ratio of the channel. The independence of the concentration profiles makes computation much easier, particularly when the dependence on the other parameters can be displayed analytically, as in perturbation expansions.

The measured current can now be predicted from Eq. 13. The resulting expression is well known but written here in explicitly microscopic variables, with A being the cross-sectional area of the pore.

$$I(V) = A \sum_i eZ_i J_i \quad (27)$$

$$I(V) = \frac{A}{d} \cdot \frac{e^2 V}{kT} \frac{1}{(1 - e^{-eV/kT})} (D_1 [C_L - rC_R e^{-eV/kT}] + D_2 [(1 - l)C_L - (1 - r)C_R e^{-eV/kT}] + D_3 [C_R - C_L e^{-eV/kT}]). \quad (28)$$

This expression yields the well known expression for the reversal potential (the potential at zero current)

$$V_{\text{rev}} = -\frac{kT}{e} \ln \frac{D_1 C_L + D_2 (1 - l)C_L + D_3 C_R}{D_1 rC_R + D_2 (1 - r)C_R + D_3 C_L}. \quad (29)$$

and the, at least as, useful (Landowne and Scruggs, 1981) expression for the short circuit (or diffusion) current

$$I(V=0) = \frac{Ae}{dT} (C_L[D_1l + D_2(1-l) - D_3] - C_R[D_1r + D_2(1-r) - D_3]). \quad (30)$$

At large transmembrane potentials $|V|$ or $|\Delta| \rightarrow \infty$, the current–voltage relation asymptotes to straight lines, passing through the origin ($I = 0$, $V = 0$)

$$I(\Delta \rightarrow +\infty) = \frac{eA}{d} \Delta [(D_1lC_L + D_2(1-l)C_L + D_3C_R) + (D_1(lC_L - rC_R) + D_2[(1-l)C_L - (1-r)C_R] + D_3(C_R - C_L))e^{-\Delta} + o(e^{-2\Delta})] \quad (31)$$

$$I(\Delta \rightarrow -\infty) = \frac{eA}{d} \Delta [(D_1rC_R + D_2(1-r)C_R + D_3C_L) + (D_1(rC_R - lC_L) + D_2[(1-r)C_R - (1-l)C_L] + D_3(C_L - C_R))e^{\Delta} + o(e^{2\Delta})], \quad (32)$$

where we use the order notation: for example, in Eq. 31, $o(e^{-2\Delta})$ means (roughly) “smaller than $e^{-2\Delta}$ as $\Delta \rightarrow +\infty$ ” (see Olver, 1974). The rectification ratio $\mathbb{R}(cf)$ measures the limiting ratio of slopes in the constant field theory and has a simple meaning if one ion is much more permeable than the other

$$\mathbb{R}(cf) \equiv \frac{\frac{\partial I}{\partial \Delta}(\Delta \rightarrow -\infty)}{\frac{\partial I}{\partial \Delta}(\Delta \rightarrow +\infty)} \rightarrow \frac{rC_R}{lC_L}, \quad \text{if } \begin{cases} D_1 \gg D_2 \\ D_1 \gg D_3 \end{cases} \quad (33)$$

The entire current–voltage relation can be sketched from these asymptotes and the reversal potential and slope there (or short circuit current and slope there; see below), because the function $I(\Delta)$ has so little structure. Evidently, its slope does not change sign: it seems to have no maxima or minima and an inflection point only at the reversal potential. Note that the accuracy of the constant field approximation may depend on the value of other parameters, e.g., the size of the transmembrane potential. For that reason we always use the numerical solution of the full set of equations (19–21) to compute results.

Slope conductance. Measurements are routinely made of current–voltage relations of open channels at different concentrations of ions. These curves are usually analyzed to show the variation with concentration of the reversal potential (the potential at which $I = 0$) and slope conductance $\partial I / \partial V|_{V=V_{\text{rev}}}$. It would be more accurate and easier (Tang et al., 1990) to measure and analyze the slope conductance at zero potential $\partial I / \partial V|_{V=0}$ because the current measured is much larger, the analytical expressions are neater, and the physical situation is simple, ions moving under their concentration but not the electrical gradient.⁵ The slope conductance at the reversal potential in a constant field

⁵When $V = V_{\text{rev}}$, the current flow through the channel is zero, but the flux of each individual ion is not zero, indeed each flux can be large, if the diffusion constants (i.e., permeabilities) are comparable.

theory is

$$\frac{\partial I}{\partial V} \Big|_{V=V_{\text{rev}}} = \frac{A}{d} \cdot \frac{e^2 V_{\text{rev}}}{kT} \cdot \frac{1}{1 - e^{-eV_{\text{rev}}/kT}} \cdot \frac{e}{kT} (D_1lC_L + D_2(1-l)C_L + D_3C_R). \quad (34)$$

The slope conductance at zero potential is

$$\frac{\partial I}{\partial V} \Big|_{V=0} = \frac{Ae}{2d} \cdot \frac{e}{kT} [D_1[lC_L + rC_R] + D_2[(1-l)C_L + (1-r)C_R] + D_3[C_L + C_R]]. \quad (35)$$

Simplifications: (case 2) long channels, with constant concentration gradient. We now turn to the more physiological case, in which the channel is longer than the width of the ionic atmosphere, that is longer than some 1 nm. Expanding Eqs. 19–21 in a power series in $1/\lambda^2$, we get for the leading terms

$$\text{Poisson equation: } \Rightarrow C_1(z) + C_2(z) - C_3(z) = 0 \quad (36)$$

$$\text{Flux equations: } \Rightarrow \begin{cases} C_1(z) + C_1(z) \cdot \Phi'(z) = -J_1 d / D_1 \\ C_2(z) + C_2(z) \cdot \Phi'(z) = -J_2 d / D_2 \\ C_3(z) - C_3(z) \cdot \Phi'(z) = -J_3 d / D_3 \end{cases} \quad (37)$$

The coupling to higher order corrections occurs through Poisson's equation but is not shown here.

Adding Eqs. 37 and 36 together and combining, gives the constant gradient in total concentration

$$\frac{d}{dz} [C_1(z) + C_2(z) + C_3(z)] = \text{constant}. \quad (38)$$

Integrating Eq. 38 and combining with Eq. 36 and the boundary conditions (21) give the concentration explicitly as a linear function of z :

$$C_3(z) = C_1(z) + C_2(z) = C_L + z \cdot (C_R - C_L) \quad 0 \leq z \leq 1. \quad (39)$$

Adding the first two equations (37), using the boundary condition (21) for Φ , we determine the nonlinear potential profile, not a constant field (in general)

$$\Phi(z) = \Delta \frac{\ln \left[z + \frac{C_L}{C_R} (1-z) \right]}{\ln \frac{C_L}{C_R}}. \quad (40)$$

Note, this implies a surface charge (from Eq. 22) of

$$\sigma_{\text{pol}}(z) = \frac{\epsilon_0 V}{a \ln \alpha} \left(\frac{\ln \left[z + \frac{C_L}{C_R} (1-z) \right]}{\ln \frac{C_L}{C_R}} - (1-z) \right), \quad (41)$$

which simplifies in the case of large or small concentration gradients to a linear gradient of surface charge. We abbreviate the ubiquitous

concentration ratio as $C = C_L/C_R$.

$$C = C_L/C_R \gg 1, \quad \sigma_{\text{pol}}(z) = \frac{\epsilon_0 V}{a \ln \alpha} z; \quad \text{for } z \neq 1$$

$$C = C_L/C_R \ll 1, \quad \sigma_{\text{pol}}(z) = \frac{\epsilon_0 V}{a \ln \alpha} (z - 1); \quad \text{for } z \neq 0. \quad (42)$$

Additional attention should be paid to the special, if not singular, cases of $|C \gg 1; z = 1|$ and $|C \ll 1; z = 0|$.

The concentrations and fluxes can now be determined by solving the equations in 37.

$$J_1 = \frac{D_1}{d} \frac{(1 - C) \left(1 + \frac{\Delta}{\ln C}\right) (rC_R - lC_L e^\Delta)}{C e^\Delta - 1} \quad (43)$$

$$J_2 = \frac{D_2}{d} \frac{(1 - C) \left(1 + \frac{\Delta}{\ln C}\right) ((1 - r)C_R - (1 - l)C_L e^\Delta)}{C e^\Delta - 1} \quad (44)$$

$$J_3 = \frac{D_3}{d} \left(\frac{\Delta}{\ln C} - 1\right) (C_R - C_L). \quad (45)$$

The concentration profiles are given by

$$C_1(z) = \frac{1}{C e^\Delta - 1} \left[(r - l) C_L e^\Delta (z(1 - C) + C) - \Delta \ln C - (rC_R - lC_L e^\Delta) (z(1 - C) + C) \right] \quad (46)$$

$$C_2(z) = \frac{1}{C e^\Delta - 1} \left[(1 - r) C_L e^\Delta (z(1 - C) + C) - \Delta \ln C - ((1 - r)C_R - (1 - l)C_L e^\Delta) (z(1 - C) + C) \right], \quad (47)$$

which determine C_3 from Eq. 39. The total electric current is then

$$I(\Delta) = \frac{C_R - C_L}{C e^\Delta - 1} \frac{eA}{d} \left[[D_1 r + D_2(1 - r) - D_3] - C e^\Delta [D_1 l + D_2(1 - l) - D_3] + \frac{\Delta}{\ln C} [D_1 r + D_2(1 - r) + D_3] - \frac{C \Delta e^\Delta}{\ln C} [D_1 l + D_2(1 - l) + D_3] \right]. \quad (48)$$

The short circuit or diffusion driven current is then the same as in the constant field case (see Eq. 30), because the electrical driving force is zero. We suspect, but have not proven, that the short circuit current is a general property of the unapproximated Eqs. 1–14, as suggested by the work of Landowne and Scruggs (1981).

At large potentials, the current–voltage relation asymptotes to straight lines that do not pass through the origin (in contrast to the constant field expressions), described by

$$I(\Delta \rightarrow +\infty) \rightarrow \frac{eA}{d} (C_L - C_R) \cdot \left[D_1 l + D_2(1 - l) - D_3 + \Delta \cdot \frac{D_1 l + D_2(1 - l) + D_3}{\ln C} \right] \quad (49)$$

and

$$I(\Delta \rightarrow -\infty) \rightarrow \frac{eA}{d} (C_L - C_R) \cdot \left[D_1 r + D_2(1 - r) - D_3 + \Delta \cdot \frac{D_1 r + D_2(1 - r) + D_3}{\ln C} \right]. \quad (50)$$

The rectification ratio $\mathbb{R}(cg)$ measures the limiting ratio of slopes in the constant gradient theory and has a simple meaning if one ion is much more permeable than the other

$$\mathbb{R}(cg) \equiv \frac{\frac{\partial I}{\partial \Delta}(\Delta \rightarrow -\infty)}{\frac{\partial I}{\partial \Delta}(\Delta \rightarrow +\infty)} \rightarrow \frac{r}{l}, \quad \text{if } \begin{cases} D_1 \gg D_2 \\ D_1 \gg D_3 \end{cases}. \quad (51)$$

Thus, at least in this case, the constant field theory predicts greater rectification than the constant gradient theory, proportional to the ratio of concentration of total salt (see Eq. 33).

The entire current–voltage relation can be sketched from these asymptotes and the reversal potential as for the constant field case. Note that the constant gradient approximation seems inaccurate when the transmembrane potential $|V|$ is large.

The slope conductance in the constant gradient theory is given below, with $\Delta_{\text{rev}} = V_{\text{rev}} e/kT$, $V_{\text{rev}} = V(I = 0)$. We hope the reader will forgive our mixing dimensionless and dimensional units for brevity's sake,

$$\frac{\partial I}{\partial V} \Big|_{V=V_{\text{rev}}} = \frac{C_R - C_L}{C e^{\Delta_{\text{rev}}} - 1} \frac{eA}{d} \frac{e}{kT} \cdot \left\{ -\frac{C e^{\Delta_{\text{rev}}}}{\ln C} (\Delta_{\text{rev}} + 1) (D_1 l + D_2(1 - l) + D_3) - C e^{\Delta_{\text{rev}}} (D_1 l + D_2(1 - l) - D_3) + \frac{D_1 r + D_2(1 - r) + D_3}{\ln C} \right\}. \quad (52)$$

The slope conductance at zero potential is

$$\frac{\partial I}{\partial V} \Big|_{V=0} = \frac{C_R - C_L}{[C - 1]^2} \cdot \frac{eA}{d} \cdot \frac{e}{kT} \cdot \mathbb{C}, \quad (53)$$

where for the sake of typography we define

$$\mathbb{C} = \frac{C}{\ln C} (r - l) (D_1 - D_2) - \frac{C^2}{\ln C} (D_1 l + D_2(1 - l) + D_3) - \frac{D_1 r + D_2(1 - r) + D_3}{\ln C} - C (D_1(r + l) + D_2(2 - r - l) - 2D_3). \quad (54)$$

Simplifications: (case 3) symmetrical concentrations, where $r = 1$. Then, the current–voltage relation is strictly linear

$$I(\Delta) = \frac{eA}{d} (C_L - C_R) \cdot \left[(D_1 r + D_2(1 - r) - D_3) + \Delta \frac{D_1 r + D_2(1 - r) + D_3}{\ln C} \right], \quad (55)$$

and so the slope conductances are equal, given by the slope of Eq. 55, namely, in dimensional units,

$$\left. \frac{\partial I}{\partial V} \right|_{V=0} = \left. \frac{\partial I}{\partial V} \right|_{V=V_{\text{rev}}} = \frac{e^2 A}{d} (C_L - C_R) \frac{D_1 r + D_2(1-r) + D_3}{k_B T \ln C}. \quad (56)$$

The (dimensionless) reversal potential can be explicitly determined

$$\Delta_{\text{rev}} = - \frac{D_1 r + D_2(1-r) - D_3}{D_1 r + D_2(1-r) + D_3} \ln C. \quad (57)$$

Simplifications: (case 4) identical diffusion constants. Equal diffusion constants in the pore $D_1 = D_2 = D_3 \equiv D$ imply a linear current-voltage relation no matter what the other parameters

$$I(V) = DV \cdot \left(\frac{eA}{d} \right) (C_L + C_R) \quad (58)$$

Simplifications: (case 5) no concentration gradient. Another special case is $C_L = C_R$, equality of total concentrations. Then, many expressions become singular and limits need to be taken as $C_L \rightarrow C_R$, giving expressions independent of the effective channel length (Arndt, Bond, and Roper, 1970). In this special case, the constant field and constant (here zero) gradient expressions are the same.

Interestingly, if the gradient of concentration is zero, one can show that the linear potential $[1-z]\Delta$ is a solution of the full set of nonlinear partial differential Eq. (1-13), suggesting that whenever the potential gradient dominates the movement of ions, a constant field will arise, except at boundary layers near $z = 0$ or 1 .

Simplifications: (case 6) no dielectric gradient. If the dielectric constant of the pore and channel wall are comparable, $\epsilon = O(1)$ as $\alpha \rightarrow 0$ and the channel is inert, as derived and described by Barcion et al. (1991). In that case, the induced charge is negligible and a constant field results. The induced charge is negligible because $(\partial\varphi/\partial r)|_{a=0,x} \approx \partial\varphi/\partial r|_{a=0,x}$; however, the radial derivatives might individually be nonnegligible.

Constant electric field and constant charge gradient. We find then (to the surprise of some of us) that a constant (electric) field is often a valid approximation: constant fields arise in all special cases that ensure small surface charge $\sigma_{\text{pol}}(z)$. In the other special case (of constant gradient), the surface charge is nearly a linear function of z .

RESULTS

The dielectric theory presented here predicts different experimental behavior in different regimes of concentration because the profiles of potential and concentration within the channel are qualitatively different in those cases. The reader more interested in experimental predictions might wish to turn directly to Fig. 6. In Results we identify those regimes and show the profiles of potential and concentration in each, along with predictions of typical experimental results. We then examine an interesting case in which channels are

predicted to be more or less in one regime for outward current and the other regime for inward current. Finally, we examine the mean field approximation and show that it applies if the electric field is spatially constant.

Different regimes: qualitative behavior. The fundamental results of an electrodiffusion theory are the profiles of concentration $C_i(x)$ and potential $\Phi(x)$ along the channel. The experimental results of current-voltage relations, slope conductance, and reversal potential are predicted from these profiles. Profiles of concentration depend on a number of parameters (although, interestingly enough, they do not depend on the diffusion constants of individual ions in the pore; see previous discussion) and so their prediction, analysis, and understanding can be complex, even when simple formulae are available.

Fig. 1 shows the regions in which different approximations and computations are valid. These regions are defined along the vertical axis by the ratio $C = C_L/C_R$ of total concentrations (of possibly permeant ions, see later definition of this term); they are defined along the horizontal axis by the effective length of the channel λ , which is inversely proportional to the Debye length and thus the square root of the ionic strength (see Eq. 17). The other parameters (e.g., membrane potential, diameter of channel, dielectric constants, diffusion constants in the pore) are held constant at physiologically reasonable values (see legend). The boundaries of the regions shown, undoubtedly depend on the values of those parameters, but that dependence has not been investigated.

Fig. 1B defines the regions more precisely for the range of parameters considered, provided the transmembrane potential Δ is not too large (Tables 1 and 2; note that setting $D_{\text{Cl}} = 0$ has no noticeable effect on any of our plotted results). The constant field expansion ($\lambda^2 \ll 1$) can be used in regions 1 and 5; the constant gradient expansion ($\lambda^2 \gg 1$) can be used in regions 3 and 4, where the channel is long compared with the Debye length. The integral equation (Barcion et al., 1991) can be used in regions 2 and 3, as well as the intermediate region 2: in region 1 it gives nearly the same results as constant field, in region 3 nearly the same as constant gradient. In region 4 the iterated solution of the integral equation does not converge. Our numerical solution of the differential equations computes so quickly (in the range of potentials reported here) that we often use it instead of the analytical approximations.

Fig. 2 describes a channel in the regime ($C_L = C_R$, long channel; cf. Table 1) where the constant field approximation should be useful. Profiles of potential

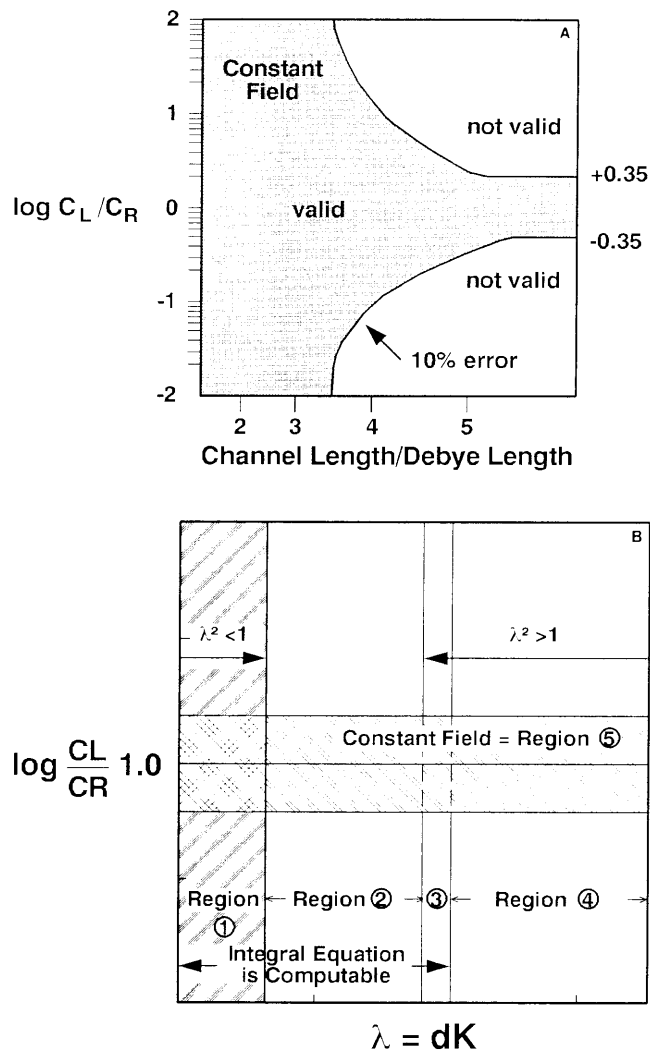


FIGURE 1 (A) Constant field approximation. The regime of validity of the constant field equation. The abscissa is the effective length λ of the channel (see Eq. 17). The ordinate is the ratio of concentration of possibly permeable ions (see text) on the left and right side of the channel. The regimes were determined rather crudely, so they are separated in the figure by a crudely drawn line; we suspect that they should be symmetrical around the line $C_L = C_R$. (B) Domains of approximation. Regions of validity of different approximations.

and concentration, and current–voltage relations (not shown) computed from the numerical algorithm are as expected from traditional analytical expressions (28–33).

Fig. 3 shows the potential (panel A) and concentration profiles (panel B) in an (effectively) long channel for a “medium” transmembrane potential (50 mV ≈ 2 kT/e) and concentration gradient (in just one direction, inside/outside = 2/1; Table 2) of possibly permeable ions. Figs. 4 and 5 show the potential (panel A) and concentration profiles (panel B) in an (effectively) long

TABLE 1 Equal total concentration of potentially permeant ions: constant field case ($C_L = C_R$)

Ion (e.g.)	Diffusion constant	Left (inside)	Right (outside)
	cm^2/s		
[K]	5×10^{-5}	150 mM = ℓC_L	3.0 mM = $r C_R$
[Na]	5×10^{-6}	30 = $(1 - \ell) C_L$	177 = $(1 - r) C_R$
[Cl]	2.5×10^{-6}	180 = $C_L = I_c$	180 = $C_R = I_c$

Setting $D_{Cl} = 0$ has no noticeable effect on any of our plotted results. Parameters: $\epsilon_\alpha = 80$; $\epsilon_m = 2$, implying $\epsilon = 0.025$; $a = 0.5$ nm; $d = 10$ nm, implying $\alpha = 0.05$, $\epsilon/(-\alpha^2 \ln \alpha) = 6.67$, and $\bar{\epsilon} = 3.338$, $\hat{I} = 1.08 \times 10^{20}$ cm^{-3} ; $\kappa^{-1} = 0.72$ nm, computed from Eqs. 16 and 17, so $\lambda = 13.9$.

channel for a “large” transmembrane potential (in both possible directions: ± 500 mV $\approx \pm 20$ kT/e) and moderate concentration gradient (Table 2) of possibly permeable ions. Note the asymmetry between Figs. 4 and 5, and the “boundary layers” (Kevorkian and Cole, 1981) emerging near $z = 0$.

Large membrane potentials. When the potential across the membrane is large compared with $kT/e \approx 25$ mV, other simplifications are needed because neither the constant field nor the constant gradient expressions are likely to be uniform approximations, valid at all membrane potentials. For this reason, experiments performed at large membrane potentials, $|\Delta| \gg 1$, are difficult to interpret with simplified theories: new effects will appear at large membrane potentials. In particular, the effects of access to a channel cannot be isolated by making measurements at large membrane potentials. Such large membrane potentials will qualitatively change behavior within the pore because they create boundary layers in the profiles of concentration and perhaps potential within the channel, boundary layers not present at smaller membrane potentials.

Current–voltage relations. The dielectric theory predicts current–voltage relations directly comparable to experi-

TABLE 2 Unequal total concentration of potentially permeant ions: constant gradient case ($C_L \neq C_R$) ($r \neq 1$)

Ion (e.g.)	Diffusion constant	Left (inside)	Right (outside)
	cm^2/s		
[K]	5×10^{-5}	600 mM = ℓC_L	180 mM = $r C_R$
[Na]	5×10^{-6}	120 = $(1 - \ell) C_L$	180 = $(1 - r) C_R$
[Cl]	2.5×10^{-6}	720 = $C_L = I_c(L)$	360 = $C_R = I_c(R)$

Setting $D_{Cl} = 0$ has no noticeable effect on any of our plotted results. Parameters: $\epsilon_\alpha = 80$; $\epsilon_m = 2$, implying $\epsilon = 0.025$; $a = 0.5$ nm; $d = 10$ nm, implying $\alpha = 0.05$ and $\bar{\epsilon} = 3.338$, $\kappa^{-1} = 0.42$ nm, computed from Eqs. 16 and 17, so $\lambda = 24$.

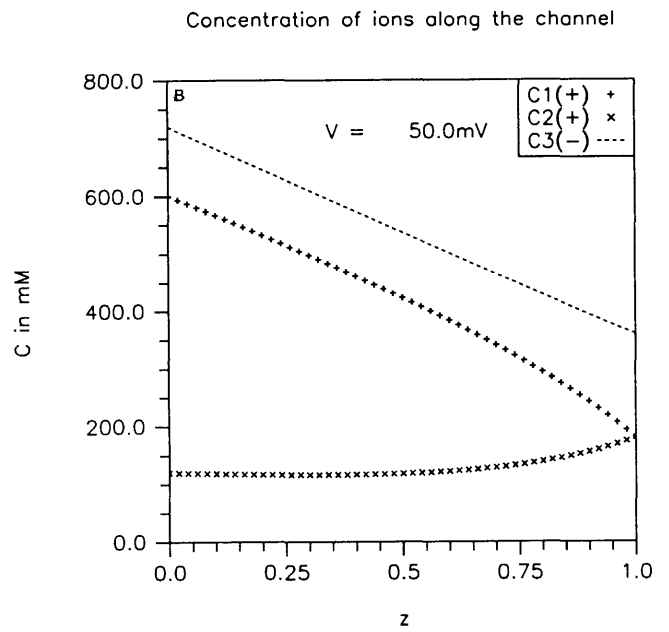
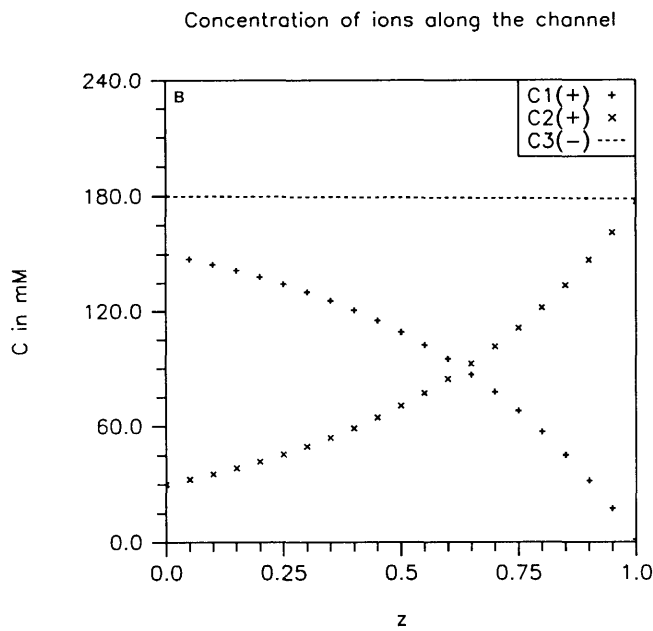
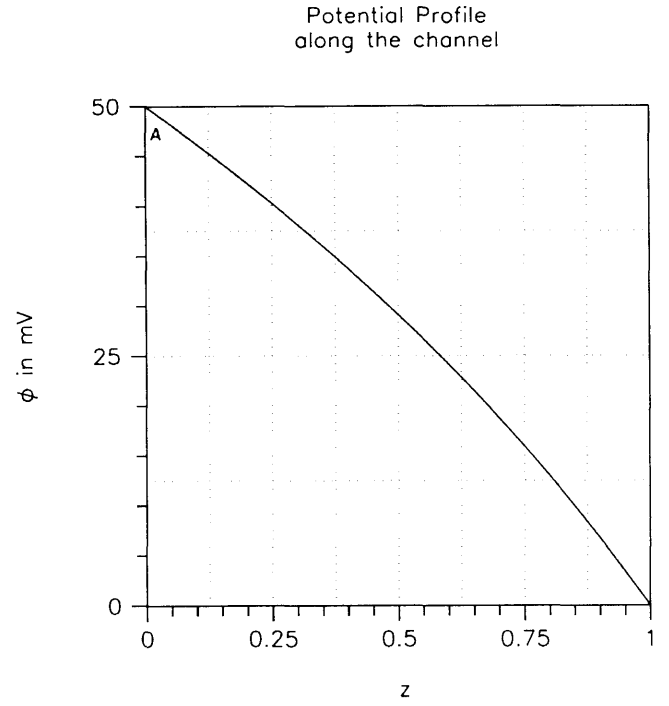
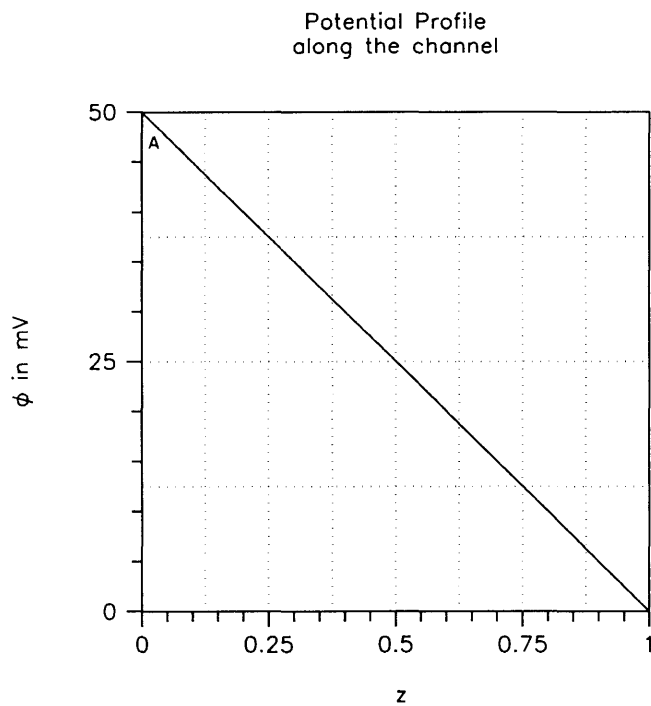


FIGURE 2 Profile of potential (A) and concentration (B) along the channel in the constant field regime, computed from the full nonlinear one-dimensional differential equations (16–22). Parameters specified in Table 1: C1 is the [K]; C2 is [Na]; and C3 is [Cl]. Setting $D_{Cl} = 0$ has no noticeable effect on any of our plotted results.

FIGURE 3 Profile of potential (A) and concentration (B) in the constant gradient regime, computed from the full nonlinear one-dimensional differential equations (16–22). Note the transmembrane potential of 50 mV. Parameters not specified or varied in figure are given in Table 2: C1 is [K]; C2 is [Na]; C3 is [Cl].

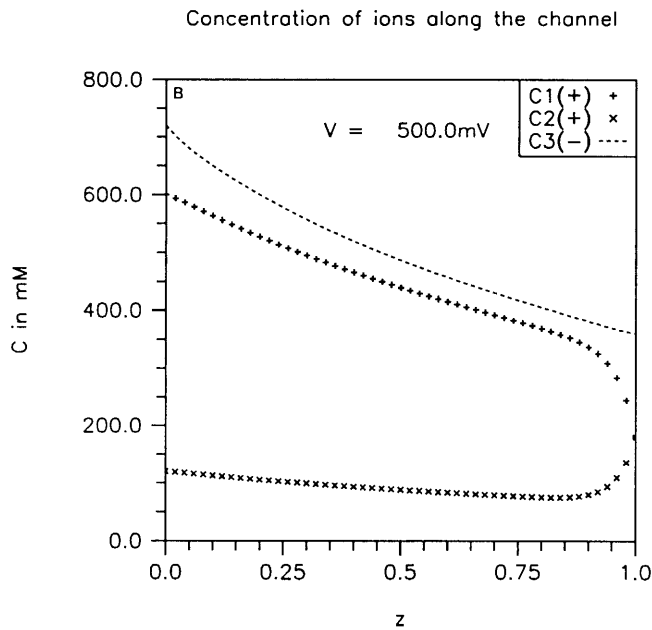
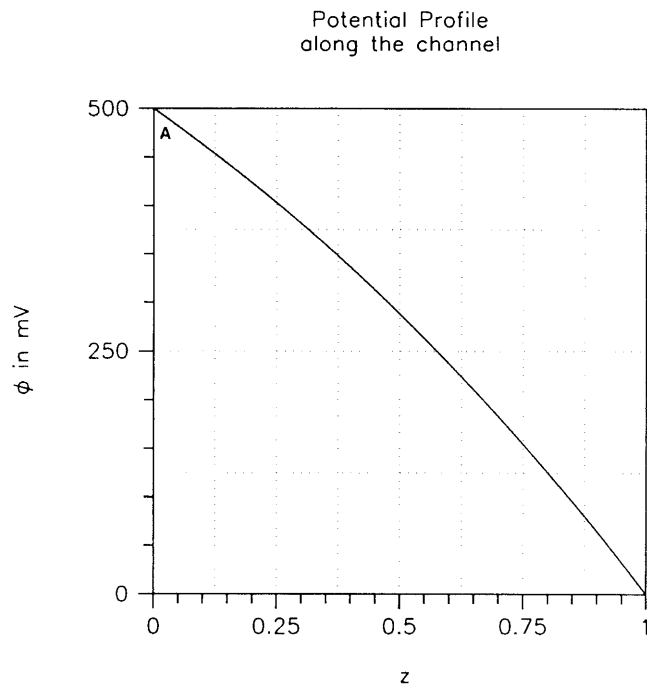


FIGURE 4 Profile of potential (*A*) and concentration (*B*) in the constant gradient regime, computed from the full nonlinear one-dimensional differential equations (16–22). Note the transmembrane potential of 500 mV. Parameters not specified or varied in figure are given in Table 2: C1 is [K]; C2 is [Na]; C3 is [Cl].

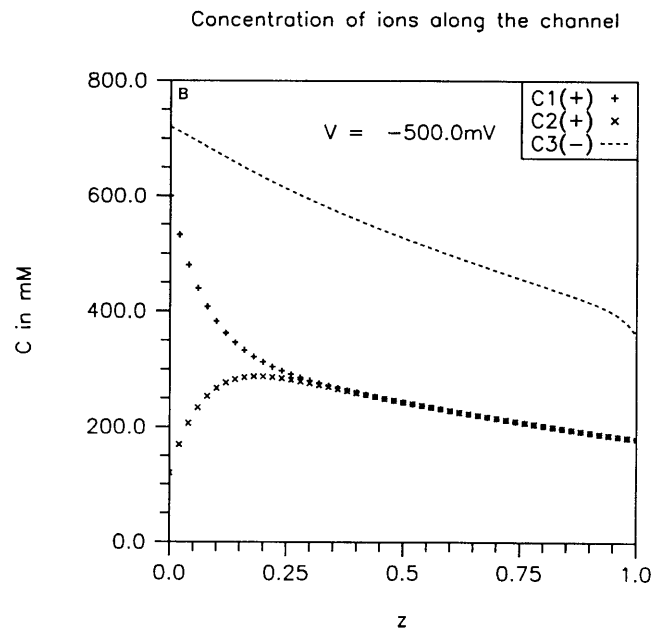
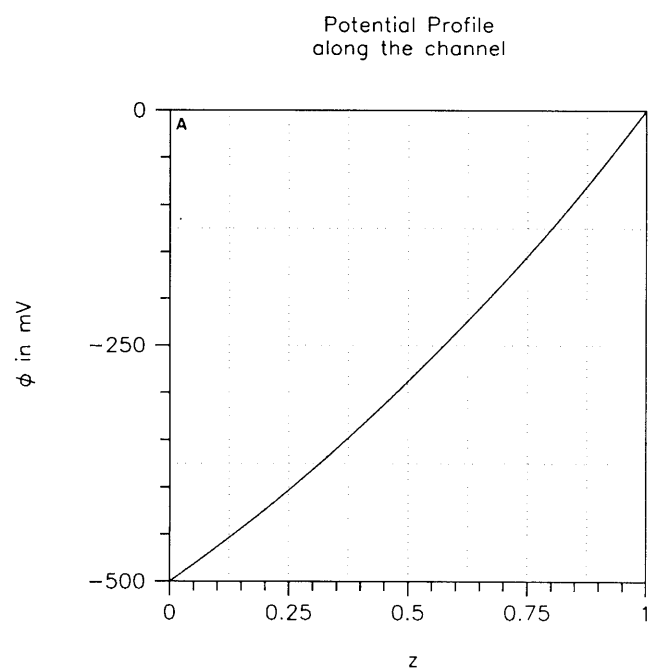


FIGURE 5 Profile of potential (*A*) and concentration (*B*) in the constant gradient regime, computed from the full nonlinear one-dimensional differential equations (16–22). Note the transmembrane potential of -500 mV. Parameters not specified or varied in figure are given in Table 2: C1 is [K]; C2 is [Na]; C3 is [Cl].

ments. Fig. 6 shows, at two different magnifications, the expected current–voltage relation for a choice of diffusion constants in the pore (Table 2) compatible with the permeability of ions found in many biological K⁺ chan-

nels. The current–voltage relation is quite close to the predictions of the constant gradient theory and quite far from that of the constant field theory, although the corresponding profiles, of $C_i(x)$ and $\phi(x)$ shown previ-

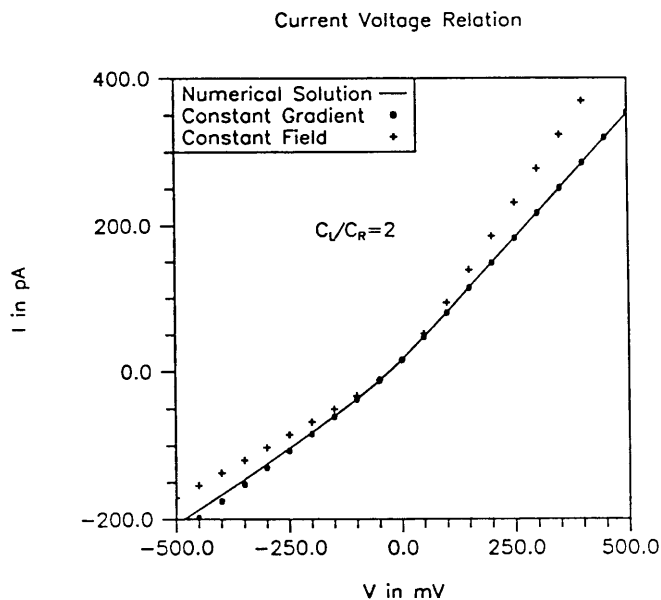


FIGURE 6 Current-voltage relation for channel (mostly) in the constant gradient regime. Parameters not specified or varied in figure are given in Table 2.

ously in Figs. 4 and 5, are not terribly far from constant field or constant gradient; it is dangerous to assume a simple graphical relation between the combination of functions in Eqs. 24–26 and the different combination in Eq. 28.

The only parameters available to determine selectivity in this dielectric theory, or constant field theory, for that matter, are diffusion constants in the pore.⁶ Anions cannot be removed entirely from the pore by setting their concentration to zero (although their diffusion constant can be set to zero) without ad hoc extensions, like selectivity filters, or large concentrations of permanent fixed charge. We choose not to make such extensions until a later paper, although we realize some may be necessary, even true; here we seek a thorough analysis of the least complicated situation, trying to avoid an *ad hoc deus ex machina* that may be inconsistent with the rest of our treatment (e.g., a selectivity filter that does not modify the electric field or the diffusion constants in the pore).

Reversal potentials. The dielectric theory predicts the reversal potential V_{rev} often used to characterize channels: channels are often exposed to varying concentrations of the most permeant ion and the measured reversal potentials are then compared with the so-called

⁶Our “diffusion constant in the pore” is simply another way of writing the “permeability” of Hodgkin and Katz (1949).

Nernst potential $V_{\text{ni}} = (kT/e) \ln [l_i C_L / (r_i C_R)]$. The reversal potential here is determined as the zero of the expression for total current (e.g., Eqs. 27, 28, or 45) using a widely available convergent root finding algorithm (Brent, 1971).

In comparing theory and experiment it is important to remember that at the reversal potential the fluxes of individual ions are not zero, nor even small, and thus analysis using thermodynamics or irreversible thermodynamics is not appropriate. Fig. 7 shows plots, in customary logarithmic format, of the $V_{\text{rev}} = (kT/e) \cdot \Delta_{\text{rev}}$ for the concentrations and diffusion coefficients of Table 1, except for the variable concentration of K^+ , the most permeable ion. We choose to vary only the external concentration of $[\text{K}^+]_0$, keeping $[\text{Na}^+]_0$ fixed, thus varying both r and C_R , thereby moving the channel out of the constant field regime. The prediction of constant field theory, for the same parameters, is shown for comparison.

It is interesting to note that the reversal potential is different in the various calculations. This should not be surprising because the reversal potential is described by different expressions in the different theories. It emphasizes once again that the reversal potential is not a thermodynamic quantity, nor is it a unique function of concentrations and diffusion constants in the pores (Patlak, 1960) derivable by, say, a general form of

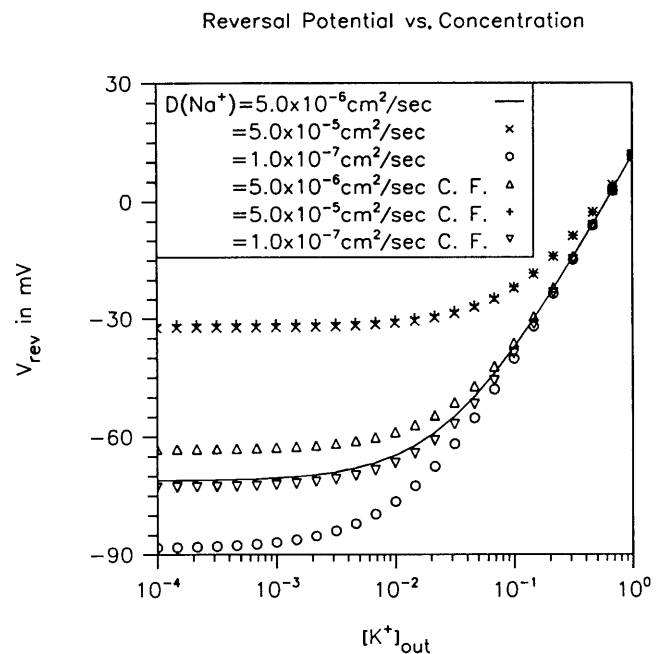


FIGURE 7 Reversal potential vs. concentration for different values of diffusion constants in the pore for Na^+ . C.F. indicates prediction of the constant field theory. Parameters not specified or varied in figure are given in Table 2.

irreversible thermodynamics independent of the geometry or dielectric constants in the problem. Rather, the expression for the reversal potential depends on the details of the kinetic model of flux through a channel.

Slope conductance. Channels are characterized by their dependence on concentration, using the slope conductance at zero current $\partial I/\partial V|_{V=V_{rev}}$ to crudely represent the entire I - V curve as concentration is varied in different ways. Fig. 8 shows plots of that slope conductance and of its close relative $\partial I/\partial V|_{V=0}$ as the concentration of K^+ and Na^+ on the outside (*right*) are varied from 1 mM to 1 M, other parameters being left as specified in Table 2. Fig. 9 shows plots of the same slope conductance for several fixed total outside concentrations C_R (= 5 mM, 150 mM, 500 mM), with the relative concentration of K^+ and Na^+ varying between zero and one. Both curves were determined from finite difference approximations to the current-voltage curves described previously. We are aware, of course, that channels often show a decreasing slope of such curves with increasing concentration, usually interpreted as a saturation phenomenon. This dielectric theory evidently does not produce such a decreasing slope and so should not be used under conditions where saturation occurs.

Moving a channel through changing regimes. It is interesting to design experiments that move a channel from one regime to another, e.g., from constant field to constant gradient, as identified in Fig. 1. Fig. 10A shows current-voltage curves in which the effective channel length is varied by changing total concentrations while the concentration ratios (r , l , and C) are held constant (at the values given in Table 2). Fig. 10B shows a plot of the reversal potential and Fig. 10C shows a plot of slope conductance vs. concentration.

Another way to vary the effective channel length keeps the concentration ratios constant on each side of the channel, but changes the ratio C_L/C_R . Fig. 10D shows current-voltage relations computed by varying C_R (and thus C_L/C_R), keeping the other parameters r and l constant at the values specified in Table 2. C_L/C_R is varied from 1 (constant field) through 10 (something like constant gradient), to (the more general case of) 100.

Experiments of this sort clearly distinguish the dielectric theory from constant field theory. Measurements made at $C_L/C_R = 1$ with varying ratios of Na^+/K^+ determine all the parameters of the constant field theory: the variation in reversal potential determines the ratio of diffusion constants, e.g., D_{Na}/D_K , and the slope conductance determines the magnitude $D_{Na} + D_K$; the value of $\bar{\epsilon}$ is not determined, however. Changing the salt gradient to $C_L/C_R = 5$ or 10 then has much less effect on the limiting current, as $V \rightarrow \infty$, of the dielectric theory

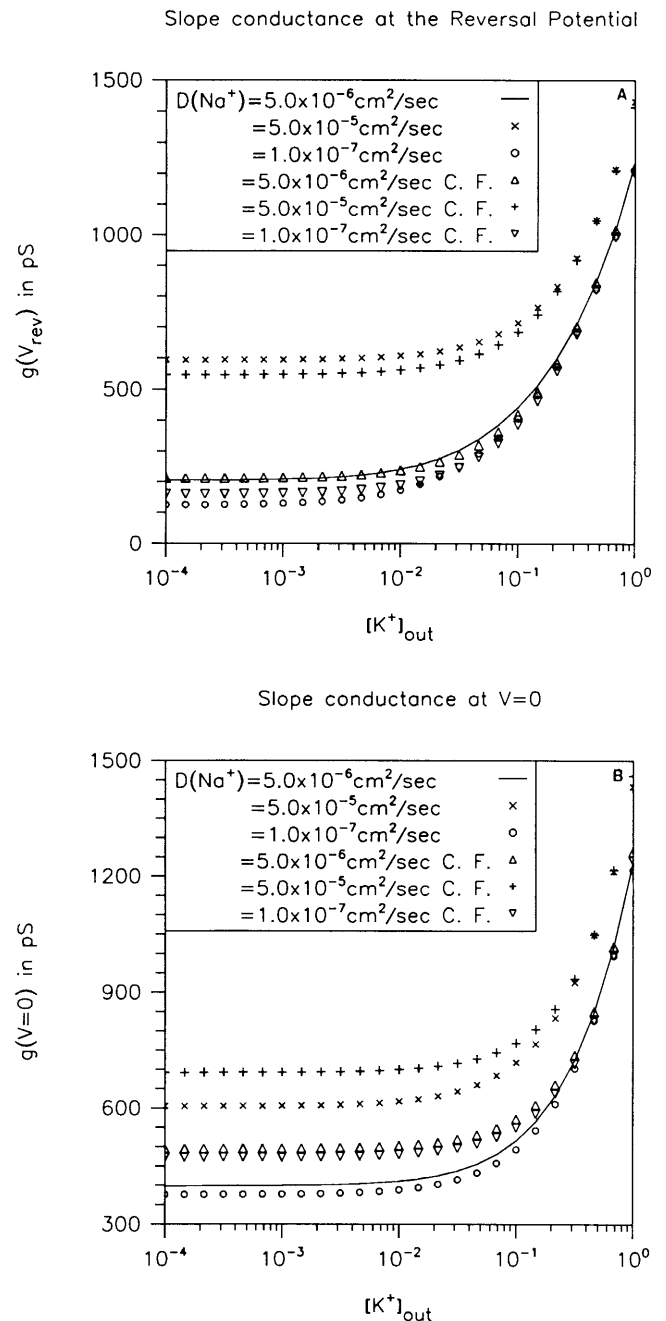


FIGURE 8 Slope conductance vs. concentration for different values of diffusion constants in pores. (A) $\partial I/\partial V|_{V=V_{rev}}$; (B) $\partial I/\partial V|_{V=0}$. Parameters not specified or varied in figure are given in Table 2.

than on the limiting current of the constant field case, as predicted by Eq. 33 and 51. Note that all the parameters of the constant field and constant gradient theory are determined by measurements at just one salt gradient C_L/C_R . No other parameters are available to fit the data taken at other salt gradients C_L/C_R in these domains.

Reversal Potential vs $[K^+]_{out}$
Fractional Concentration

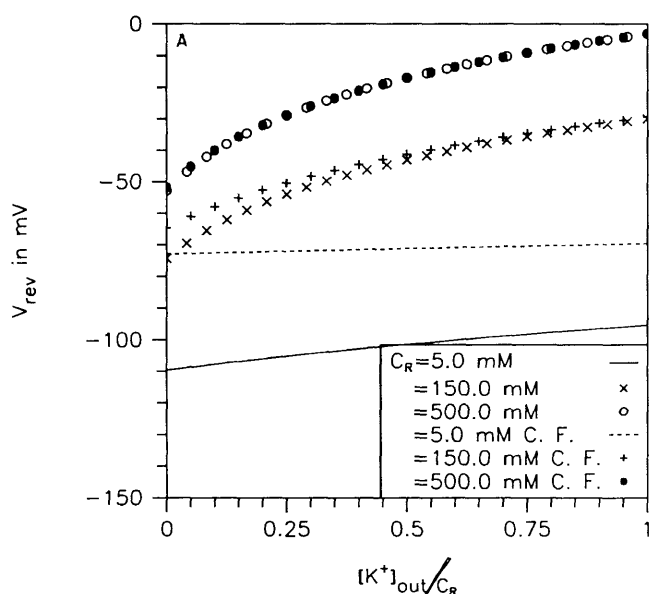
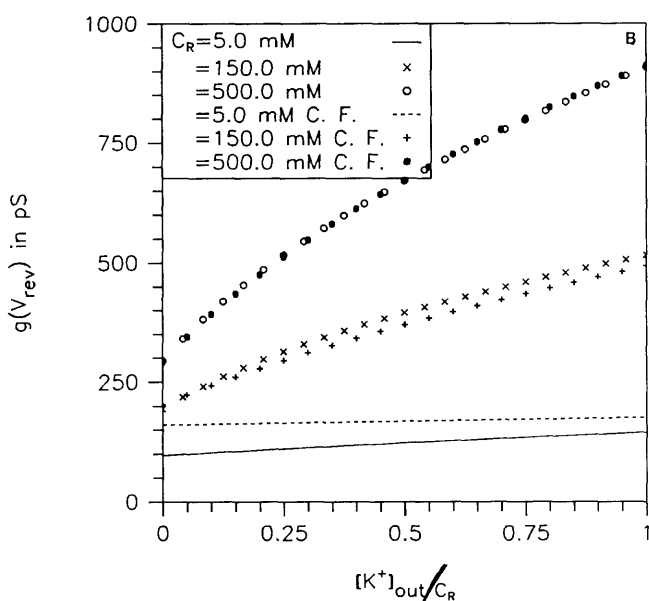
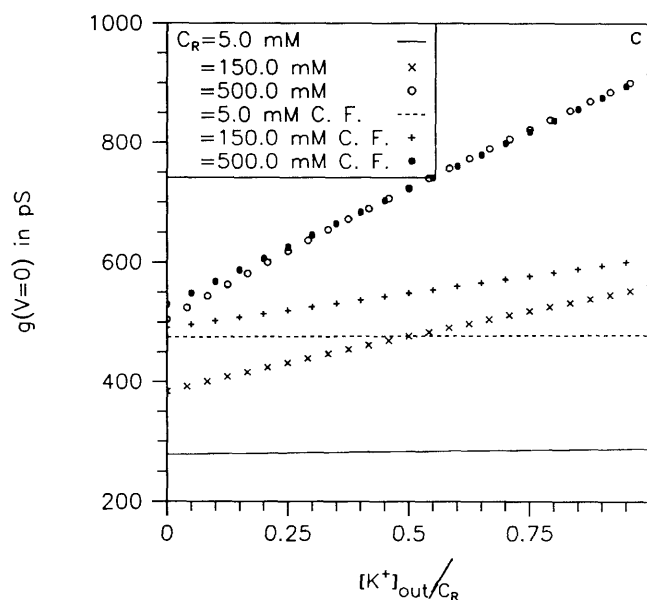


FIGURE 9 Reversal potential (A) and slope conductance (B and C) as a function of the fractional concentration (*abscissa*). Parameters not specified or varied in figure are given in Table 2.

Slope conductance at the Reversal Potential



Slope conductance at V=0



Only one parameter, $\bar{\epsilon}$, is available to fit data taken in other domains and the predictions seem a weak function of this parameter.

Fig. 11 shows an interesting calculation for a different set of parameters $[K]_{in} = \ell C_L = 300$ mM, $[Na]_{in} = (1 - \ell)C_L = 60$; $[K]_{out} = rC_R = 18$, $[Na]_{out} = (1 - r)C_R = 18$; the current-voltage relation shifts regimes as it shifts quadrant. When current is positive (outward) and potential is positive (depolarizing), the curve is close to

constant gradient, evidently dominated by the high internal concentration $C_L = 360$ mM. When the current is negative (inward) and the potential is negative (hyperpolarizing), the curve is close to constant field, evidently dominated by the low external concentration $C_R = 36$.

In all these calculations, the diffusion constants in the pore D_i are held constant, independent of concentration. The concentration dependence of current-voltage curves shown here is a consequence of the complex

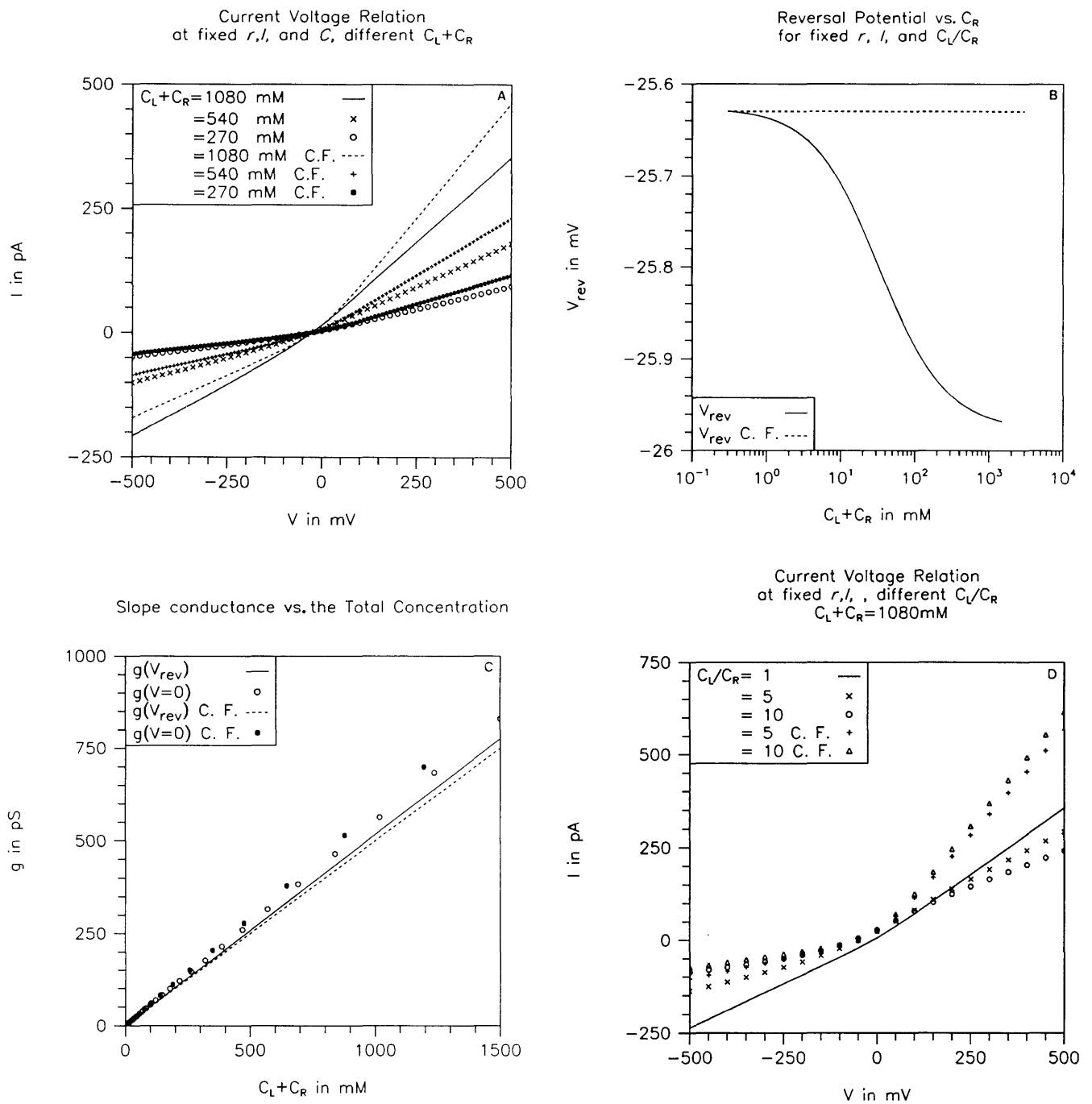


FIGURE 10 Moving channels from one regime to the other by changing concentrations: current–voltage relations (*A* and *D*) and derived quantities (reversal potential (*B*) and slope conductance (*C*)). Note the large difference between constant field and constant gradients in *D*; this should be easy to detect in experimental data. Parameters not specified or varied in figure are given in Table 2.

interactions of ions and channel, not of a variation in the frictional interactions (i.e., permeabilities) of ions.

The interaction potential. The potential describing the interaction between an ion and the channel wall (i.e., the

potential on the cylindrical surface of the channel $\varphi(r = a \pm 0)$, is not in general a constant: the charge $\sigma_{pol}(z)$ induced on the channel wall depends on all the parameters of the problem (see Eqs. 14 and 22). In many theories, however, the interaction potential $\varphi(r = a \pm 0)$

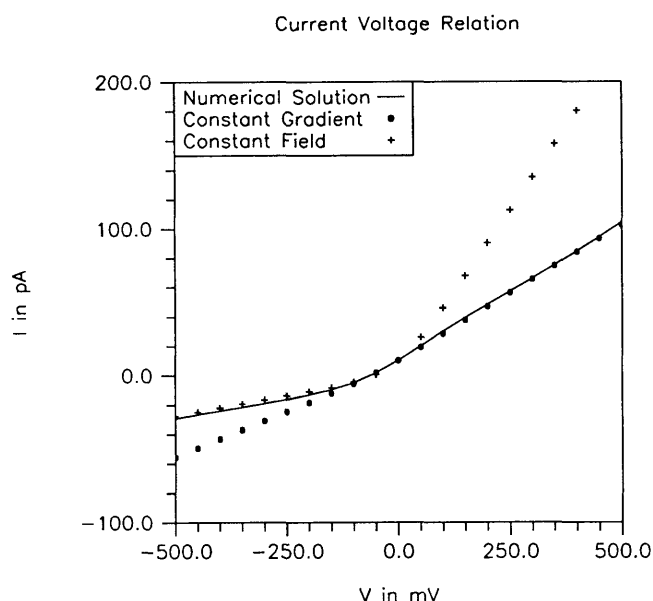


FIGURE 11 Current-voltage relation for a large concentration gradient. Note that the current-voltage relation (solid line: numerical solution) approximates that of the constant field approximation when current flow is inward (negative) and that of the constant gradient approximation when current flow is outward (positive). Parameters are:

	Diffusion constant	Left (inside)	Right (outside)
	cm ² /s		
[K]	5×10^{-5}	300 mM = ℓC_L	18 mM = $r C_R$
[Na]	5×10^{-6}	60 = $(1 - \ell)C_L$	18 = $(1 - r)C_R$
[Cl]	2.5×10^{-6}	360 = C_L	36 = C_R

Setting $D_{Cl} = 0$ has no noticeable effect on any of our plotted results. Parameters not specified or varied in figure or this caption are given in Table 2.

is assumed constant, independent of other parameters and dependent variables.

Most mean field theories approximate the interaction of an ion with the channel wall by the deviation $\mathcal{S}(z, \Delta)$

$$\mathcal{S}(z, \Delta) \equiv \Phi(z) - [1 - z]\Delta = \sigma_{\text{pol}}(a \ln \alpha)(e/[\epsilon_0 k T]), \quad (59)$$

the difference between the total potential and the constant field potential at this location, proportional to the induced charge (see Eqs. 14, 20, and 22). As long as $\Phi(z)$ nearly equals $\Delta \cdot [1 - z]$, a channel is in the constant field regime, with $\mathcal{S}(z, \Delta) \approx 0$, $\sigma_{\text{pol}}(z) \approx 0$, independent of Δ . Then, the ion does interact with a channel protein with an invariant profile of potential, a constant field, i.e., a potential linear in x . In this sense then the classical constant field theory turns out to be

the mean field theory of channology, the theory with no induced charge, as one should have expected a priori, but did not.

When channels do not contain a spatially constant electric field, however, the mean field approach is often inappropriate, because the induced charge is often substantial and variable. Fig. 12 shows the deviation $\mathcal{S}(\frac{1}{2}, \Delta)$ of the potential from constant field in the middle of the channel ($z = \frac{1}{2}$) as a number of parameters are changed. For example, panel A shows the deviation as a function of the transmembrane potential for various concentrations with the parameters of Table 2 (cf. Eqs. 41, 42). Panel B shows the deviation $\mathcal{S}(\frac{1}{2}, \Delta)$ as a fraction of the transmembrane potential. The deviation $\mathcal{S}(\frac{1}{2}, \Delta)$ is not constant in most cases, showing that the interaction of ion and channel wall usually cannot be described as the interaction of an ion with a fixed potential, except when the channel is in the constant field regime (when the deviation remains zero, of course).

Panel C shows one case, however, in which the deviation (i.e., induced surface charge) is nearly constant; the deviation does not depend significantly on \bar{e} (that is to say, it does not depend on the ratio of dielectric constants, or the ratio of length to diameter) for the parameters of Table 2. There is at least one other case in which the interaction between an ion and a channel is constant, even if the interaction is large and the electric field is not constant; we have previously shown (e.g., Eqs. 23–26 and 40, 46, 47) that the potential and concentration profiles within the channel do not depend on the diffusion constants (i.e., permeabilities) of individual ions in the pore (see earlier discussion).

Thus, we see that mean field theories can be used for the range of parameters considered here (Table 1 and 2) when the channel is in the constant field regime, or the parameters varied are the dielectric constants, diameter or length of the channel, or diffusion constant of ions in the pores. Otherwise, a mean field theory is likely to be inappropriate.

DISCUSSION

Historical notes. Barcilon, Chen, and Eisenberg (1991) describe ionic motion in the pore by a system of nonlinear differential equations and boundary conditions not previously analyzed, to the best of our knowledge. Levitt, 1978, 1985, 1986, 1988; Peskoff and Bers, 1988; and Jordan and his colleagues (e.g., Jordan, 1982, 1983, 1984, reviewed in Jordan, 1987; Jordan et al., 1989) have emphasized the importance of electrostatic

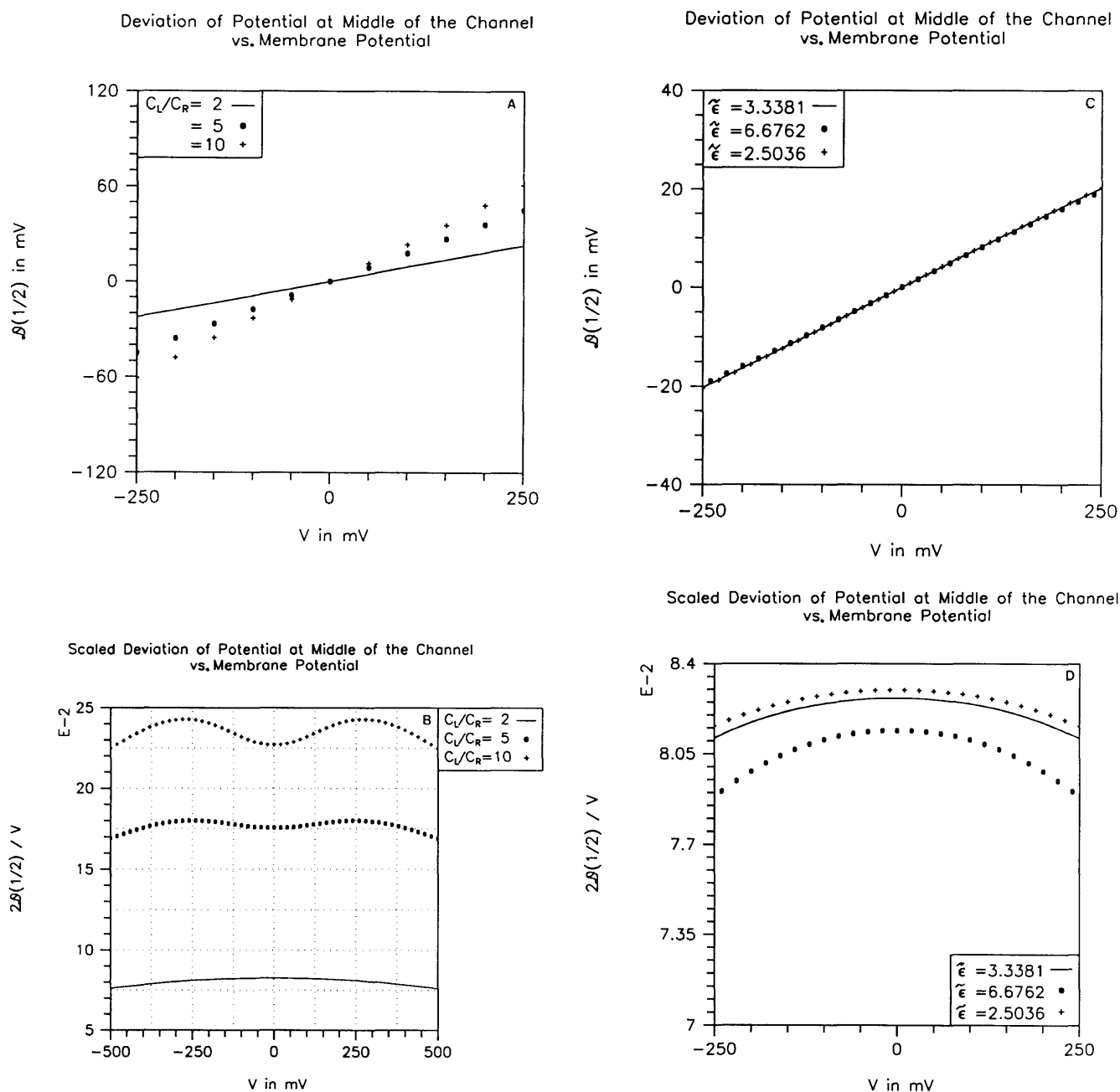


FIGURE 12 Deviation of potential in the middle of the channel for constant field, shown in absolute (*A* and *C*) and relative units (*B* and *D*) for different concentration ratios (*A* and *B*) or (ratios of) dielectric constants and (ratios *f*) channel length and area (*C* and *D*). Parameters not specified or varied in figure are given in Table 2.

interactions in ionic channels,⁷ but have not tried to analyze flux through a pore in a protein, i.e., a hole in a dielectric. Bass, 1964; Zelman, 1968; MacGillivray, 1968;

⁷Our theory computes the electrostatic interaction under many conditions and presents it as the potential $\Phi(z)$. The cited literature computes the $J_i = 0$ case with various approximations.

MacGillivray and Hare, 1969; Friedman, 1969; Zelman and Shih, 1972; de Levie and Moreira, 1972; de Levie, Seidah, and Moreira, 1972; Lauger and Neumcke, 1973; Jackson, 1974; Mafe, Pellicer, and Aguilera, 1986; and Riveros, Croxton, and Armstrong, 1989, have emphasized the importance of the violation of electrical neutrality, the space charge that accompanies ionic diffusion,

but have not studied its interaction with a surrounding dielectric.

Barcilon et al. (1991) analyze current flow, allowing violation of electrical neutrality and interaction with a dielectric, using a continuum description of ionic motion in the pore. The ions in the pore interact electrically, but only electrically, with the channel wall; the net charge in the pore induces charge in the channel wall. Analysis and approximation leads to a one-dimensional integro-differential equation (Eq. 5.17 of Barcilon et al., 1991), of considerable complexity, that can be formulated as a system of nonlinear ordinary differential equations (Eqs. 19 and 20) or as an equivalent integral equation (Eqs. 5.18–5.20 of Barcilon et al.). Each formulation is quite involved, so it is a welcome surprise that their numerical evaluation can yield simple curves, reminiscent of the properties of real channels and classical theories.

The body of this paper shows how the simple curves come about. Numerical analysis yields simple curves over a wide range of parameters. Ionic movement can occur in a constant electric field for a limited range of concentrations and potentials. It is only under those conditions that a mean potential theory should be applied.

In the general case, and probably in the biological situation, the electric field is not constant; in channels nanometers long, in solutions of more than a few millimolar ionic strength, the electric field varies with location. The gradient of the *total* concentration of all permeant ions, however, can, for some potentials and concentration gradients, be nearly constant in such channels, as assumed for the case of zero flux by Planck (1890a, b; see MacInnes, 1961, pp. 461–465). The other classical (Henderson) assumption of the liquid junction potential is, however, not accurate; the gradient of concentration of each ion is not constant, as assumed by Henderson (1907; see MacInnes, 1961, pp. 231–233). Interestingly, the results of the constant field and constant gradient theories are indistinguishable in an important special case, when the gradient of the total concentration of permeant ions is zero (Arndt, Bond, and Roper, 1970). Then, the zero concentration gradient is accompanied by a constant electric field, *independent of channel length or ionic strength*. If the gradient of total concentration is even a factor of two, however, the constant field theory is not very accurate.

Limitations of our model. The analysis presented here is of a reduced but reasonable model with more or less the dimensions of the gramicidin pore. It is not meant to describe our current view of a specific biological channel, both because that view may prove ephemeral, and because our hope is to uncover qualitative phenomena

and properties common to many channel types, helpful in the design and interpretation of experiments.

The physical model is mesoscopic, not atomic and not macroscopic. The parameters of the model clearly need to be understood in terms of the atomic parameters of molecular dynamics, but it will take some effort and time (human and machine) to stretch present day simulations (some 0.1 ns in duration) into the biological time scale of micro- and milliseconds. Meanwhile, a hierarchy of models needs investigation: atomic dynamics, to determine atom–atom interactions, including induced charge; molecular dynamics, to determine the permeating path, potential of mean force, and motions of the channel protein; Langevin simulations and stochastic differential equations to follow ions interacting with each other moving through channels; Fokker-Planck equations, to analyze the first-passage time of noninteracting ions; finally, the Nernst-Planck equations of this paper, to describe the steady-state flux. Each level of the hierarchy is needed to provide the parameters for the next: the potential functions of molecular dynamics come from study of atom-atom interactions; the friction (i.e., memory kernel) of Langevin dynamics comes from molecular dynamics; the potential barriers and diffusion constants of the stochastic differential equations, Nernst-Planck; and Fokker-Planck equations come from the potential of mean force determined in molecular and/or Langevin dynamics.

Such an hierarchical approach will take some time to complete so we can fully understand our mesoscopic variables. But physical insight (i.e., guesses) can help in the mean time. For example, the mean concentration in the pore is a mesoscopic variable depending on stochastic quantities. Clearly it is in some sense the average number of ions in a channel in some time period, determined by the instrumentation used to record current, divided by that time period and the volume of the channel. Thus, concentration in the pore depends on more than just the spatial distance between ions, it also depends on the arrival rate and transit time of the ion and the bandwidth of the instrumentation. Concentration in the pore, thus, has quite a different meaning from concentration in a bulk solution.

The mathematical limitations of our analysis also need mention. Error analysis of matched asymptotic expansions is an active field of mathematical research and is often impossible or impractical. The only known way to determine the errors in expansions like ours is numerical; the problem is too nonlinear, allowing too many combinations of parameters, to allow convincing general analysis. For that reason, we are currently working on a numerical solution of the full field equations. We know how to check such a calculation and which range of parameters to study because of the

analysis presented here. Indeed, without prior asymptotic analysis our computer would drown our reason in a sea of numbers.

Possibly permeant ions. A possibly permeant ion is one that maintains its steady-state concentration profile during the time interval of measurement (from 10 μ s to 1 s) clearly long enough to justify our assumption of steady-state. Ions that do not enter channels in this time period should be excluded from the computation of C_L or C_R . Our analysis concerns only possibly permeant ions. Ions that are partially excluded from the channel (in this time period) cannot be treated by our theory but are easily recognized in experimental records. Such ions enter the channel but do not reach their stationary concentration during its open interval. They contribute a varying current and produce a "sloping top" on the observed single channel current, if they contribute significantly to the current at all. Single channel records rarely show a systematic drift in the current through an open channel.

The theoretical analysis of Cohen and Cooley (1965) suggests that K^+ , Na^+ , and Cl^- ions reach their steady concentration in nanoseconds. Thus, the mobility of an ion would need to be reduced by a factor of 10^4 to produce observable nonstationary phenomena, in which case the ion would carry immeasurable current; experimentally, mobilities need to be some 2% of free solution values to yield resolvable currents and to make an ion "possibly permeable."

The preceding paragraphs ignore the so-called liquid junction potentials between the bath containing impermeable ions and the solution within the channel excluding the absolutely impermeable ions. The d.c. potential so created is hopefully small, and can in any case be dealt with as an offset by the usual experimental methods of electrochemistry and electrophysiology.

Experimental tests. The best use of the dielectric model and theory presented here is the design of experiments, experiments to test the theory, experiments that might otherwise not be done. For example: (a) current-voltage relations can be measured in the constant field domain $C_L = C_R$ for enough ratios of concentration $[Na^+]/[K^+]$ to determine the ratio of diffusion constants D_{Na}/D_K (from measurements of reversal potential) and $D_{Na} + D_K$ (from measurements of slope conductance), just as has been done in traditional experiments for many decades; (b) a salt gradient can then be imposed, moving the channel to the constant gradient regime (e.g., see Table 2 and Fig. 10) and measurements made at any and all convenient concentrations; (c) the channel can then be moved to a mixed regime (e.g., see Fig. 11) and

measurements made once more at any or all convenient concentrations; and finally, (d) the gradient C_L/C_R used in either the constant gradient or mixed domain can be maintained while reducing the ionic strength (i.e., C_L and C_R) so the channel is in effect shortened, moving it to still another domain where constant fields should exist for all realizable concentrations. The dielectric theory predicts all current-voltage relations for regimes 2-4, along with any others and any other concentration gradients, from the measurements in just the first constant field regime, without recourse to adjustable parameters.

When a theory is this specific, predicting so many results under so many conditions, without possibility of adjustment, it is so constrained that it will probably fail. Its authors are, thus, wise to choose an escape path, even before experiments force them into it. Clearly, we have no shortage of escapes; open channel conduction should depend on a number of phenomena not included in our dielectric theory, viz. (a) permanent surface charge on the channel protein, (b) the entry process from bath to pore, (c) the distinct diameter of different ions, (d) ion-ion interactions. A model is likely to need some of these effects to make a fitting, let alone convincing theory of open channel permeation and ion selectivity. Some of these effects can be included using the mathematical apparatus of this dielectric theory, but others probably require the hierarchy of analysis previously mentioned.

APPENDIX

The averaged channel

The dielectric theory described here is derived in Barcion et al. (1991) using the theory of matched asymptotic expansions (Kevorkian and Cole, 1981) to exploit the narrow aspect ratio present in at least some channels. Because this theory is unfamiliar to some readers, we thought it worthwhile to present another approach to show what can be derived by averaging, and what requires the full asymptotic analysis.

Define the average concentration $C_i(z)$, the average potential $\Phi(z)$ within the pore, and the average potential outside the pore $\psi(z)$, in the channel protein and membrane, remembering that, in this Appendix, the aspect ratio $\alpha(z) \equiv a(z)/d$ is a function of z although we do not write the functional dependence explicitly.

$$\begin{aligned}
 C_i(z) &\equiv \frac{2}{\alpha^2} \int_0^{a(z)} r c_i(r, z) dr \\
 \Phi(z) &\equiv \frac{2}{\alpha^2} \int_0^{a(z)} r \phi(r, z) dr \\
 \psi(z) &\equiv \frac{2}{\alpha^2} \int_{a(z)}^{\infty} r \cdot \phi dr. \tag{A1}
 \end{aligned}$$

The averaged Nernst-Planck equations are derived by combining Eq. 1 and 2, multiplying by $2r$ and integrating from $r = 0$ to $r = a$.

$$\frac{dC_i}{dz} + Z_i C_i \cdot \frac{d\Phi}{dz} = -J_i d/D_i. \quad (\text{A2})$$

A full asymptotic analysis is needed to see if other significant terms arise from writing the product of average values as the average of the products and from the cavalier treatment of $\alpha(z)$ here and below.

The averaged Poisson's equation within the pore is

$$\frac{d^2\Phi}{dz^2} + \frac{2}{\alpha^2} \frac{\partial\Phi}{\partial r}(a-0, z) = -\lambda^2 \sum_i Z_i C_i; \quad r < a. \quad (\text{A3})$$

Turn now to the region $r > a$, outside the pore, namely the channel wall and surrounding membrane, described by Eq. 4 with boundary conditions (Eq. 9 and 10). After multiplication by r and integration from $r = a$ to $r = \infty$, the averaged Laplace's equation is

$$\alpha^2 \frac{d^2\psi}{dz^2} - 2 \frac{\partial\Phi}{\partial r}(a+0, z) = 0 \quad r > a, \quad (\text{A4})$$

because the radial dependence $\partial\Phi/\partial r$ disappears far from the channel, as $r \rightarrow \infty$. The induced surface charge σ_{pol} can be written from Eq. 10 and 14 of the text.

$$\sigma_{\text{pol}} = \frac{\epsilon_0 kT}{ea(z)} \left[\frac{\partial\Phi}{\partial r}(a-0) - \frac{\partial\Phi}{\partial r}(a+0) \right] \quad (\text{A5})$$

$$= -\frac{\epsilon_0 kT}{ea(z)} \cdot \frac{1-\epsilon}{\epsilon} \cdot \frac{\partial\Phi}{\partial r}(a-0) \quad (\text{A6})$$

$$= \frac{\epsilon_0 kT}{ea(z)} \cdot (\epsilon-1) \cdot \frac{\partial\Phi}{\partial r}(a+0). \quad (\text{A7})$$

Combine (A4) and (A7) to write

$$\sigma_{\text{pol}} = \frac{\epsilon_0 kT}{2ea(z)} (\epsilon-1) \alpha^2 \frac{d^2\psi}{dz^2} \quad r > a. \quad (\text{A8})$$

Combine (A3) and (A6) to write

$$\frac{d^2\Phi}{dz^2} + \frac{2\epsilon}{\epsilon-1} \frac{ea(z)}{\epsilon_0 kT \alpha^2} \sigma_{\text{pol}} = -\lambda^2 \sum_i Z_i C_i \quad r < a. \quad (\text{A9})$$

A full analysis of the potential outside the pore is needed to determine σ_{pol} and proceed further. The potential in the channel protein $\phi(a+0, z)$ can be determined from Laplace's equation for the potential in the channel wall $\phi(r > a)$ (Eq. 4 in text) with the far field boundary condition $\phi(r \rightarrow \infty; z) \rightarrow (1-z)\Delta$. Barcilon et al. (1991), particularly its Appendix, solve that problem. After the Bessel function $K_0(n\pi\alpha r)$ of the far field has been expanded for small arguments (Eqs. A.8, A.9, and A.18–A.27), leaving $1/(-\ln\alpha)$ as its trace, the induced charge can be determined from Eqs. A.30 and 5.16 (Barcilon et al).

$$\sigma_{\text{pol}}(z) = \frac{\epsilon_0 kT}{ea(z)} \cdot (1-\epsilon) \frac{1}{\ln\alpha} [\Phi - (1-z)\Delta]. \quad (\text{A10})$$

This reduces to Eq. 22 if we remember that the ordering of $\bar{\epsilon}$, ϵ , and α in Barcilon et al. (1991) implies that $\epsilon \ll 1$.

The potential inside the pore can now be expressed by replacing the

induced charge σ_{pol} of Eq. A8 with the results (A10) of the expansion for $r > a$. The resulting modified Poisson equation is test Eq. 20.

$$\frac{d^2\Phi}{dz^2} - \frac{2\epsilon}{-\alpha^2 \ln\alpha} [\Phi - (1-z)\Delta] = -\lambda^2 \sum_i Z_i C_i. \quad (\text{A11})$$

The average potential $\psi(z)$ outside the pore is related to the average potential $\Phi(z)$ within the pore: compare σ_{pol} of Eqs. A9 and A10.

$$-(\alpha^2 \ln\alpha) \frac{d^2\psi}{dz^2} = \Phi(z) - (1-z)\Delta = \mathcal{S}(z, \Delta). \quad (\text{A12})$$

We see then that the deviation $\mathcal{S}(z, \Delta)$ from the longitudinal constant field within the pore is produced by the second longitudinal derivative of the average potential outside the channel, which is, of course, proportional to the induced charge σ_{pol} (see Eq. 22).

The constant field term $(1-z)\Delta$ in our dielectric theory describes the potential within the membrane far from the channel, where the dielectric properties of the membrane are uniform and the potential is entirely electrostatic, unperturbed by diffusion, migration, or space charge. The constant field spreads towards the channel wall through Laplace's Eq. 4, as shown by the matching of asymptotic expansions in Barcilon et al (1991). The constant field term spreads into the pore through boundary condition 9, perturbed in the average potential as shown in Eq. A12. There, in the pore it meets and matches constant field terms that arise from the nonlinear Nernst-Planck equations themselves (independent of the dielectric) under special conditions, e.g., when the gradient of total concentration is zero, or the channel is short. Constant fields arise in many contexts in this problem, but they only dominate in some.

The averaged quantities of this Appendix can describe the mean properties of a pore that has variable cross-section and is as long as wide; thus, it seems that dielectric theory describes the averaged properties of many channels.

Conversations with Mark Ratner were a joy and a help throughout this work. Fred Cohen, Tom DeCoursey, Stuart McLaughlin, Fred Quandt, and Eduardo Rios kindly provided vigorous and useful criticism of the manuscript.

We are grateful for the steadfast support of the National Science Foundation.

Received for publication 22 April 1991 and in final form 6 December 1991.

REFERENCES

- Adrian, R. H. 1969. Rectification in muscle membrane. *Prog. Biophys. Mol. Biol.* 19:341–369.
- Arndt, R. A., J. D. Bond, and D. L. Roper. 1970. An exact constant-field solution for a simple membrane. *Biophys. J.* 10:1149–1153.
- Barcilon, V., D. P. Chen, and R. S. Eisenberg. 1991. Ion flow through narrow membrane channels. *Siam J. Appl. Math.* In press.
- Bass, L. 1964. Electrical structures of interfaces in steady electrolysis. *Trans. Faraday Soc.* 60:1656–1663.
- Brent, R. P. 1971. Algorithm with guaranteed convergence for finding a zero of a function. *Comp. J.* 14:422–425.
- Brooks, C. L., M. Karplus, and B. M. Pettitt, 1988. Proteins: A Theoretical Perspective of Dynamics, Structure, and Thermodynamics. John Wiley & Sons, New York. 259 pp.

- Buck, R. P. 1984. Kinetics of bulk and interfacial ionic motion: microscopic bases and limits for the Nernst-Planck equation applied to membrane systems. *J. Membr. Sci.* 17:1-62.
- Cohen, H., and J. W. Cooley. 1965. The numerical solution of the time-dependent Nernst-Planck equations. *Biophys. J.* 5:145-162.
- Cole, K. S. 1965. Electrodiffusion models for the membrane of squid giant axon. *Physiol. Rev.* 45:340-379.
- Cole, K. S. 1968. *Membranes, Ions and Impulses*. University of California Press, Berkeley, CA. 568 pp.
- Cooper, K. E., P. Y. Gates, and R. S. Eisenberg. 1988. Surmounting barriers in ionic channels. *Quart. Rev. Biophys.* 21:331-364.
- Cooper, K. E., E. Jakobsson, and P. Wolynes. 1985. The theory of ion transport through membrane channels. *Prog. Biophys. Mol. Biol.* 46:51-96.
- Feynmann, R. P., R. B. Leighton, and M. Sands. 1963. *Feynmann Lectures on Physics*, Vol. 2. Addison-Wesley, New York.
- Friedman, M. H. 1969. On an analysis of the constant field equation. *J. Theor. Biol.* 25:502-504.
- Goldman, D. E. 1943. Potential, impedance, and rectification in membranes. *J. Gen. Physiol.* 25:37-60.
- Henderson, P. 1907. Zur thermodynamik der flüssigkeitsketten. *Zeitschrift für Physikalische Chemie.* 59:118-128.
- Henderson, P. 1908. Zur thermodynamik der flüssigkeitsketten. *Zeitschrift für Physikalische Chemie.* 63:325-345.
- Hess, K. 1988. *Advanced Theory of Semiconductor Devices*. Prentice Hall, NJ. 268 pp.
- Hille, B. 1984. *Ionic Channels of Excitable Membranes*. Sinauer Associates Inc., Sunderland, MA.
- Hodgkin, A. L. 1971. *The Conduction of the Nerve Impulse*. Liverpool University Press, Liverpool. 108 pp.
- Hodgkin, A. L. 1977. Chance and design in electrophysiology: an informal account of certain experiments on nerve carried out between 1934 and 1952. In *The Pursuit of Nature*. Hodgkin, A. L., Huxley, A. F., Feldberg, W., Rushton, W. A. H., Gregory, R. A., and McCance, R. A., editors. Cambridge University Press, London. 1-22.
- Hodgkin, A. L., and B. Katz. 1949. The effect of sodium ions on the electrical activity of the giant axon of the squid. *J. Physiol.* 108:37-77.
- Israelachvili, J. N. 1985. *Intermolecular and Surface Forces*. Academic Press, London, p. 26.
- Jackson, J. L. 1974. Charge neutrality in electrolytic solutions and the liquid junction potential. *J. Phys. Chem.* 78:2060-2064.
- Jordan, P. C. 1982. Electrostatic modeling of ion pores. Energy barriers and electric field profiles. *Biophys. J.* 39:157-164.
- Jordan, P. C. 1983. Electrostatic modeling of ion pores. II. Effects attributable to the membrane dipole potential. *Biophys. J.* 41:189-195.
- Jordan, P. C. 1984. Effect of pore structure on energy barriers and applied voltage profiles. I. Symmetrical channels. *Biophys. J.* 45:1091-1100.
- Jordan, P. C. 1987. Microscopic approaches to ion transport through transmembrane channels. The model system gramicidin. *J. Phys. Chem.* 91:6582-6591.
- Jordan, P. C., R. J. Bacquet, J. A. McCammon, and P. Tran. 1989. How electrolyte shielding influences the electrical potential in transmembrane ion channels. *Biophys. J.* 55:1041-1052.
- Kevorkian, J., and J. D. Cole. 1981. *Perturbation Methods in Applied Mathematics*. Springer-Verlag, New York, NY.
- Kramers, H. A. 1940. Brownian motion in a field of force and the diffusion model of chemical reactions. *Physica.* 7:284-304.
- Landowne, D., and V. Scruggs. 1981. Effects of internal and external sodium on the sodium current-voltage relationship in the squid giant axon. *J. Membr. Biol.* 59:79-89.
- Läuger, P., and B. Neumcke. 1973. Theoretical analysis of ion conductance in lipid bilayer membranes. In *Membranes*, Vol. 2. George Eisenman, editor. Marcel Dekker, New York, NY. p. 51
- de Levie, R., and H. Moreira. 1972. Transport of ions of one kind through thin membranes. I. General and equilibrium considerations. *J. Membr. Biol.* 9:241-260.
- de Levie, R., N. G. Seidah, and H. Moreira. 1972. Transport of ions of one kind through thin membranes. II. Nonequilibrium steady-state behavior. *J. Membr. Biol.* 20:171-192.
- Levitt, D. G. 1978. Electrostatic calculations for an ion channel. I. Energy and potential profiles and interactions between ions. *Biophys. J.* 22:209-219.
- Levitt, D. G. 1982. Comparison of Nernst-Planck and reaction-rate models for multiply occupied channels. *Biophys. J.* 37:575-587.
- Levitt, D. G. 1985. Strong electrolyte continuum theory solution for equilibrium profiles, diffusion limitation, and conductance in charged ion channels. *Biophys. J.* 52:575-587.
- Levitt, D. G. 1986. Interpretation of biological ion channel flux data. Reaction rate versus continuum theory. *Annu. Rev. Biophys. Biophys. Chem.* 15:29-57.
- Levitt, D. G. 1988. Electrostatic radius of the gramicidin channel determined from voltage dependence of H⁺ ion conductance. *Biophys. J.* 53:33-38.
- MacGillivray, A. D. 1968. Nernst-Planck equations and the electroneutrality and donnan equilibrium assumptions. *J. Chem. Phys.* 48:2903-2907.
- MacGillivray, A. D., and D. Hare. 1969. Applicability of Goldman's constant field assumption to biological systems. *J. Theor. Biol.* 25:113-126.
- MacInnes, D. A. 1961. *The Principles of Electrochemistry*. Dover, New York, NY. 478 pp.
- Mafe, S., J. Pellicer, and V. M. Aguilera. 1986. Ionic transport and space charge density in electrolytic solutions as described by Nernst-Planck and Poisson equations. *J. Phys. Chem.* 90:6045-6050.
- Mafe, S., J. A. Manzanares, and J. Pellicer. 1988. The charge separation process in non-homogeneous electrolyte solutions. *J. Electroanal. Chem.* 241:57-77.
- Markowich, P. A. 1986. *The Stationary Semiconductor Device Equations*. Springer-Verlag, New York. 193 pp.
- McCammon, J. A. and S. C. Harvey. *Dynamics of Proteins and Nucleic Acids*. Cambridge, New York. 234 pp.
- Murthy, C. S., and K. Singer. 1987. Description of the molecular trajectories in simple liquids. *J. Phys. Chem.* 91:21-30.
- Neumcke, B., and P. Lauger. 1969. Nonlinear electrical effects in lipid bilayer membranes. II. Integration of the generalized Nernst-Planck equations. *Biophys. J.* 9:1160-1170.
- Olver, F. W. J. 1974. *Asymptotics and Special Functions*. Academic Press, New York. 572 pp.
- Panofsky, W., and M. Phillips. 1962. *Classical Electricity and Magnetism*. Second Edition. Addison-Wesley. 32. 39-43.
- Patlak, C. S. 1960. Derivation of an equation for the diffusion potential. *Nature (Lond.)*. 188:944-945.
- Peskoff, A., and D. M. Bers. 1988. Electrodiffusion of ions approaching the mouth of a conducting membrane channel. *Biophys. J.* 53:863-875.
- Planck, M. 1890a. Ueber die Erregung von Electricität und Wärme in Electrolyten. *Annalen der Physik und Chemie. Physik.* 39:161-186.

-
- Planck, M. 1890b. Annalen der physik und chemie. Ueber die Potentialdifferenz zwischen zwei verdünnten Lösungen binärer Electrolyte. *Annalen der Physik und Chemie*. 40:561–576.
- Press, W. H., B. P. Flannery, S. A. Teukolsky, and W. T. Vetterling. 1986. *Numerical Recipes*. Cambridge University Press, New York.
- Purcell, E. M.. 1985. *Electricity and Magnetism*, 2nd Ed. McGraw-Hill, New York. 484 pp.
- Riveros, O. J., T. L. Croxton, and W. McD. Armstrong. 1989. Liquid junction potentials calculated from numerical solutions of the Nernst-Planck and Poisson equations. *J. Theor. Biol.* 140:221–230.
- Rubinstein, I. 1990. *Electro-Diffusion of Ions*. Society for Industrial and Applied Mathematics, Philadelphia. 249 pp.
- Selberherr, S. 1984. *Analysis and Simulation of Semiconductor Devices*. Springer-Verlag, New York. 293 pp.
- Sewell, G. 1982. *IMSL Software for Differential Equations in One Space Variable*. IMSL Technical Report Series, No. 8202, IMSL, Houston. 1–15.
- Sten-Knudsen, O. 1978. Passive transport processes. In *Membrane Transport in Biology: Concepts and Models*, Vol. 1. D. C. Tosteson, editor. Springer-Verlag, New York. 5–113.
- Tang, J. M., J. Wang, F. N. Quandt, and R. S. Eisenberg. 1990. Perfusing pipettes. *Pflügers Arch.* 416:347–350.
- Verhoeven, J. 1963. Electrotransport in metals. *Metallurg. Rev.* 8:311–368.
- Zelman, D. A. 1968. An analysis of the constant field equation. *J. Theor. Biol.* 18:396–398.
- Zelman, D. A., and H. H. Shih. 1972. The constant field approximation: numerical evaluation for monovalent ions migrating across a homogeneous membrane. *J. Theor. Biol.* 37:373–383.